North American Journal of Economics and Finance 69 (2024) 102022

Contents lists available at ScienceDirect

North American Journal of Economics and Finance

journal homepage: www.elsevier.com/locate/najef

A hybrid approach of wavelet transform, ARIMA and LSTM model for the share price index futures forecasting

Junting Zhang [a], Haifei Liu [a,*], Wei Bai [a], Xiaojing Li [b]

[a] School of Management and Engineering, Nanjing University, Nanjing 210093, China
[b] ICBC Jiangsu Branch, Nanjing 210093, China

ARTICLE INFO

JEL Classification:
G29

Keywords:
DWT-ARIMA-LSTM
Harr wavelet-based porous algorithm
Share price index futures
Timing trading strategy

ABSTRACT

In this study, a novel hybrid model for share price index futures forecasting named WT-ARIMA-LSTM is proposed. In this hybrid model, share price index futures are decomposed to extract data characteristics at different time scales by the wavelet transform and the ARIMA-LSTM model are applied to predict the close price of futures. The findings of the study are as follows. 1) The DWT hybrid model and the MODWT hybrid model have higher forecasting accuracy than some commonly used forecasting models under the three metrics of MAE, MAPE and RMSE. The DWT-ARIMA-LSTM model has better forecasting performance when the forecasting performance in different markets and the operational efficiency of the method are combined. 2) The DWT method is more applicable than the MODWT method in forecasting models of futures closing price series; the approximate signals obtained from the DWT decomposition have lower volatility and can better characterise the original signals. 3) The LSTM model has better prediction performance for noisy residual series, while the ARIMA model has better prediction performance for less noisy approximate signals. 4) Based on the forecasting results, a timing trading strategy is constructed that can maintain a robust return performance under different market conditions, especially on the risk side with significant advantages. In addition, this work examines the impact of the unexpected event of the COVID-19 epidemic on the forecasting performance of the model, and the results show that the model can adapt to different data structures to achieve more robust forecasting performance. This work provides insights into the integration of deep learning methods with econometric methods in the field of asset pricing.

1. Introduction

Futures markets, similar to most financial markets, are dynamic, complex and highly volatile and irregular (Hou & Li, 2020). Many classical asset price forecasting theories and models have been proposed, but few of them perform well as futures prices are affected by many volatile factors, including macroeconomic conditions, market contingencies and traders, and the data exhibit a complex structure. Therefore, the subject of asset price forecasting has been immensely attractive and challenging.

The methods for stock index futures forecasting can be roughly categorized into four types: traditional forecasting methods, econometric model forecasting methods, artificial intelligence methods and hybrid model forecasting methods. Traditional forecasting

* Corresponding author at: School of Management and Engineering, Nanjing University, No.5 Pingcang Lane, Gulou District, Nanjing, Jiangsu Province, Post code: 210093, China.

E-mail addresses: hfliu@nju.edu.cn (H. Liu), 2226376292@qq.com (X. Li).

https://doi.org/10.1016/j.najef.2023.102022
Received 18 September 2022; Received in revised form 4 August 2023; Accepted 10 October 2023
Available online 14 October 2023
1062-9408/

methods mainly include fundamental analysis and technical analysis (Ahmad et al., 2017; Choi, 1995; G, C. 2012).Technical analysis depends on the subjective judgement of investors, making it difficult to achieve effective forecasts in the long term (Phuong & L., & Cam Nhung, V. , 2021; Islam, Ghafoor, & Eberle, 2018; Juszczuk, Kozak, & Kania, 2020; Phooi & M'ng, J., & Mehralizadeh, M. , 2018).

Econometric models and artificial intelligence methods are currently the dominant research methods for asset price forecasting. Econometric models have better performance in dealing with linear relationships, with ARIMA models being most vastly used for time series forecasting, while econometric models are limited by excessive model assumptions and difficult to handle non-linear relationships (Chortareas, Jiang, & Nankervis, 2011; Joo & Kim, 2015). Artificial intelligence methods, such as artificial neural networks (Dunis & Huang, 2002; Tsang et al., 2007; Wright, 2008), recurrent neural networks, and long and short-term memory networks (Shi & Chehade, 2021), can compensate for the lack of ability to deal with non-linear relationships in econometric methods. Deep learning model has better processing and feature extraction capabilities for complex structured data (G. Zhang, Eddy Patuwo, & Y. Hu, 1998). However, due to the high level of noise in financial data, AI methods are often prone to model overfitting (Hu, Zhang, Jiang, & Patuwo, 1999; G. Zhang, Eddy Patuwo, Hu, & M., 1998). In general, traditional forecasting methods are better understood, more accessible and more acceptable to investors. Econometric models and artificial intelligence models have different conditions of applicability, with econometric models being better at dealing with linear relationships and artificial intelligence models better at capturing the non-linear features of the series (Persio & Honchar, 2016; Rather, Agarwal, & Sastry, 2015; Weytjens, Lohmann, & Kleinsteuber, 2021).

To sum up, combining two different models tends to achieve better forecasting than using a single model (Lv, Wu, Xu, & Shu, 2022; G. P. Zhang, 2003). Bates and Granger (1969) first demonstrated that the forecasting error of a linear combination of multiple feasible models was smaller than that of the benchmark model in the component (Bates & Granger, 1969). Subsequently, an increasing number of hybrid models have been applied to asset price forecasting problems (Ghahnavieh, 2019; Kim & Won, 2018; Rahimi & Khashei, 2018).

Although the approach of the combination of linear and non-linear models in hybrid models proof its potential in improvement of forecasting relative to the classical model, there are still some significant shortcomings in the aforementioned hybrid models. One of the limitations of the models is that it is difficult to extract features from different time scales of the data due to the the complex structure of financial data and the amount of noise it contains (Wang & m., & Wu, C. , 2010). Investors in the market have different preferences. Some investors tend to hold stocks for the long term and the price movements caused by their investment behavior have a long-term memory, while others are used to short-term operations and are prone to short-term price movements (Stevenson, 1998; Sun & Meinl, 2012). The presence of investors with different investment philosophies and risk appetites in the same financial market can cause asset prices to exhibit multiple price fluctuations overlaid on the same time scale (Bekiros, Arreola Hernandez, Salah Uddin, & Muzaffar, 2020; Shik Lee, 2004). Therefore, the features of financial data need to be effectively analyzed and extracted first before modelling. Combining data decomposition with forecasting models to forecast asset prices is an effective forecasting framework, specifically combining data decomposition methods such as wavelet decomposition and EMD with forecasting models such as ARMA models, ARIMA models, ARIMA-GARCH models, SVM models, Tree-based machine learning methods and LSTM models (Chen, Lai, & Sun, 2019; Joo & Kim, 2015; Liu & Huang, 2021; Lv, Shu, Xu, & Wu, 2022; Pai & Lin, 2005; Phooi M'ng, 2018; Sadorsky, 2022; Zhu & Wei, 2013; Zolfaghari & Gholami, 2021). It can be concluded from previous studies that: firstly, the lack of effective data processing leads to a significant decrease in the predictive performance of the forecasting models; secondly, econometric models such as ARMA and ARIMA can effectively capture the seasonal characteristics of the data while fitting non-seasonal data less effectively, and therefore the predictive performance of ARIMA models is poor in certain data sets; finally, the data decomposition techniques can effectively improve the forecasting of model which indicates that data decomposition techniques can provide effective data cleaning and feature extraction for financial data.

Another of the limitations of the models is the feature selection for deep learning model. Technical analysis indicators are the most common criteria in quantitative investments for predicting the price movement of assets (Neely, Rapach, Tu, & Zhou, 2014; Phooi & M'ng, J., & Mehralizadeh, M. , 2018). Firstly, technical indicators are based on market trading data, and thus technical indicators naturally contain the necessary market information; secondly, technical indicators measure investors' beliefs about financial assets and reflect information such as momentum in the market (Phuong & L., & Cam Nhung, V. , 2021; Huang, Li, Wang, & Zhou, 2020; Novy-Marx, 2012); finally, it has been suggested that technical analysis is essentially noise deal and therefore technical analysis indicators represent the behavioral characteristics of a dominant noise traders group in the market that uses technical analysis as a guide to investment (Neely et al., 2014). It can be concluded that technical analysis indicators are not sufficient to achieve effective forecasting but provide information about changes in momentum and noise deal, so incorporating technical analysis indicators into model training features can be effective in improving model forecasting performance (Islam, Ghafoor, & Eberle, 2018; Juszczuk et al., 2020).

The most relevant research work is Lin, Yan, Xu, Liao, and Ma (2021) combining CEEMDAN method with LSTM model to improve the applicability of the models to financial data (Y. Lin et al., 2021). This paper utilizes a new mixture model that combines CEEMDAN with LSTM to forecast stock index price. Unlike their approach, the hybrid model which combines the ARIMA model with the LSTM model, has a better fit for the time series than the single model to compensate for the shortcomings of both in this work.

In addition, unlike the previous practice of decomposing data and then filtering for noise (Phooi & M'ng, J., & Mehralizadeh, M. , 2016; F.-L. Lin, Yang, Marsh, & Chen, 2018; Sun, Chen, & Yu, 2015), Neely argued that there are a large number of noise traders in the market and that in some markets noise traders are dominant (Neely et al., 2014). Thus, extraction-free harr wavelets in wavelet decomposition are applied to ensure the integrity of the decomposition sequence information and indicators of technical analysis are added to the feature engineering of the LSTM model to characterize the noise as well as momentum information in the market to further improve the predictive power of the LSTM model.

In this work, an ARIMA-LSTM forecasting model combining with the wavelet transform is proposed to forecast the closing price of stock index futures based on the idea of decomposition-forecasting-reconstruction. In this model, wavelet analysis is applied to decompose the futures closing price data into low-frequency long-term trend terms and high-frequency short-term fluctuation terms. The ARIMA model is applied to initially fit the time series, capture the linear relationship of the time series and obtain the forecasting error term, which includes mainly the non-linear relationship between the data. Then, the LSTM model is employed to process the non-linear relationship in the ARIMA forecasting error term to further reduce the forecasting error. Finally, the forecasting results of the hybrid model are obtained by synthesizing the low-frequency and high-frequency forecasting sequences. Extensive experiments are conducted on ten representative share price index futures. The experimental results showed that our proposed model outperforms other reference models in term of forecasting accuracy.

The main contributions of this work are as follows:

(1) This paper proposes a hybrid WT-ARIMA-LSTM model, which shows excellent forecasting performance in stock index futures forecasting and outperforms the forecasting model proposed by Lin et al. (Y. Lin et al., 2021). The prediction model is also applied to a real investment problem to construct a time-timing strategy, which achieves higher returns and maintains lower risk in back testing compared to the buy-and-hold strategy.

(2) The introduction of wavelet decomposition effectively solves the problem of more noise in financial time series data as pointed out by Neely (Neely et al., 2014) and improves the feature extraction ability of the model for financial time series data. Extraction-free Haar wavelets are applied in wavelet decomposition to ensure the completeness of the information in the decomposed sequence, and the original sequence is decomposed into low-frequency and high-frequency sequences to characterize the long-term trends and noisy trading behaviors in the financial market.

(3) The experiments provide evidence for comparing the predictive ability of traditional econometric models and deep learning models on financial data. For noisy sequences, the deep learning model has better prediction performance, while for less noisy sequences, the traditional econometrics model is able to achieve similar or even better prediction results than the deep learning model, which complements the study of Persio and Weytjens(Persio & Honchar, 2016; Weytjens et al., 2021).

The rest of this paper is organized as follows. Section 2 presents the framework of wavelet transform, CEEMDAN, ARIMA, LSTM, hybrid model and the proposed prediction model. Section 3 presents the empirical analysis and results, mainly including the wavelet decomposition and CEEMDAN decomposition results, and the prediction results of the hybrid model. Section 4 introduces the timing trading strategy based on the prediction results in Section 3; Section 5 presents the robustness tests, which examine the robustness of the strategy under different quotes and the impact of COVID-19 epidemic shock on the stability of the strategy. Finally, Section 6 summarizes the conclusions.

2. Research design

To predict share price index futures, the methodology employed in this work follows a hybrid approach, namely, the WT-ARIMA-LSTM. This section summarizes the main components of the hybrid models including: (1) Wavelet transform, (2) Maximal overlap discrete wavelet transform, (3) Complete EEMD with adaptive noise, (4) ARIMA, (5) LSTM and (6) Hybrid model.

2.1. Wavelet transform

Wavelet transform is commonly applied to decompose a signal into a set of basic functions of the signal. Discrete wavelets (DWT), in which the multi-resolution analysis proposed by Mallat is commonly used, is vastly applied in time series forecasting. However, DWT is not time-shift invariant due to its sampling of the signal while the $\grave{\alpha}$ trous algorithm is time-shift invariant and can be applied well in time series forecasting (Høg, 2001). Therefore, in this study, we use the $\grave{\alpha}$ trous algorithm proposed by M. Shen and use the Haar wavelet as the wavelet basis for wavelet transform.

For the time series f(t), DWT calculates the scale factor with a low-pass filter as the following:

$$c_0(t) = f(t) \tag{1}$$

$$c_{j+1}(t) = \sum_{m=-\infty}^{\infty} h(m) c_j\left(t + 2^j m\right) \tag{2}$$

The detail factor can be calculated from the scale factor as the following:

$$d_{j+1}(t) = c_j(t) - c_{j+1}(t) \tag{3}$$

Thus, the wavelet decomposition of the original series with resolution q is $\{d_1, d_2, \cdots, d_q, c_q\}$, where, $d_j (j = 1, 2, \cdots q)$ stands a fine signal in j level and c_q stands for an approximate signal. The time series can be reconstructed as follows:

$$f(t) = c_q(t) + \sum_{j=1}^{q} d_j(t) \tag{4}$$

In this study, we use $h = \left(\frac{1}{2}, \frac{1}{2}\right)$ as the low-pass filter, so c_j and d_j can be restated as:

$$c_{j+1}(t) = \frac{1}{2}\left(c_j\left(t - 2^j\right) + c_j(t)\right) \tag{5}$$

$$d_{j+1}(t) = c_j(t) - c_{j+1}(t) \tag{6}$$

2.2. Maximal overlap discrete wavelet transform (MODWT)

MODWT is an improvement of the discrete wavelet transform. Modwt has no requirement for signal length during signal decomposition and reconstruction, making it more versatile in its application(Sun & Meinl, 2012).

Assuming that the length of the time series $\{X_i\}$ is N, the MODWT of the wavelet and scale coefficients is defined as follows.

$$\widetilde{W}_{jt} = \sum_{l=0}^{L-1} \widetilde{h}_{jt} \bullet X_{t-1 modN} \tag{7}$$

$$\widetilde{V}_{jt} = \sum_{l=0}^{L-1} \widetilde{g}_{jt} \bullet X_{t-1 modN} \tag{8}$$

where $\widetilde{h}_{jt}$ and $\widetilde{g}_{jt}$ denote the wavelet filter and scale filter of the jth layer of MODWT, respectively. The wavelet filter $\widetilde{h}_{jt}$ and the scale filter $\widetilde{g}_{jt}$ are defined as follows.

$$\widetilde{h}_{jt} = h_{jt} \Big/ 2^{j/2} \tag{9}$$

$$\widetilde{g}_{jt} = g_{jt} \Big/ 2^{j/2} \tag{10}$$

2.3. Complete EEMD with adaptive noise (CEEMDAN)

CEEMDAN is an improved algorithm based on the CEEMD algorithm, which can effectively solve the problem of transferring white noise from high to low frequencies in the CEEMD algorithm.

Let $E_i(\bullet)$ be the i − th eigenmode component after EMD decomposition, $\overline{\mathrm{C_i(t)}}$ be the i − th eigenmode component obtained by CEEMDAN decomposition, v^j be the Gaussian white noise satisfying the standard normal distribution, $j = 1, 2, \cdots, N$. $y(t)$ is the signal to be decomposed.

The Gaussian white noise is introduced into the signal to be decomposed, and the EMD decomposition of the signal is performed to obtain the first-order eigenmodal component C_1 as follows.

$$E\left(y(t) + (-1)^q \varepsilon v^j(t)\right) = C_1^j(t) + r^j, q = 1, 2. \tag{11}$$

The first eigenmodal component of the CEEMDAN decomposition and the residuals are obtained by overall averaging of the generated N modal components.

$$\overline{C_1(t)} = \frac{1}{N} \sum_{j=1}^{N} C_1^j(t) \tag{12}$$

$$r_1(t) = y(t) - \overline{C_1(t)} \tag{13}$$

The new signal is obtained by adding positive and negative paired Gaussian white noise to the residual term $r_1(t)$, and the EMD decomposition is performed to obtain the first − order modal component D_1^j and the overall average is performed to obtain the 2nd eigenmodal component and residual of the CEEMDAN decomposition.

$$\overline{C_2(t)} = \frac{1}{N} \sum_{j=1}^{N} D_1^j(t) \tag{14}$$

$$r_2(t) = r_1(t) - \overline{C_2(t)} \tag{15}$$

The above steps are repeated until the residual term is a monotonic function. Assuming that the number of eigenmodal components is K, the original signal $y(t)$ is decomposed as follows.

$$y(t) = r_k(t) + \sum_{k=1}^{K} \overline{C_k(t)} \tag{16}$$

2.4. ARIMA

The ARIMA model was proposed by Box et al. It is essentially an extension of the autoregressive moving average model (ARMA). ARMA model requires the time series to satisfy stationary, which is almost impossible in practice. Therefore, differencing is used to remove the non-stationary of the series. The general structure of ARIMA (p, d, q) model is as follows:

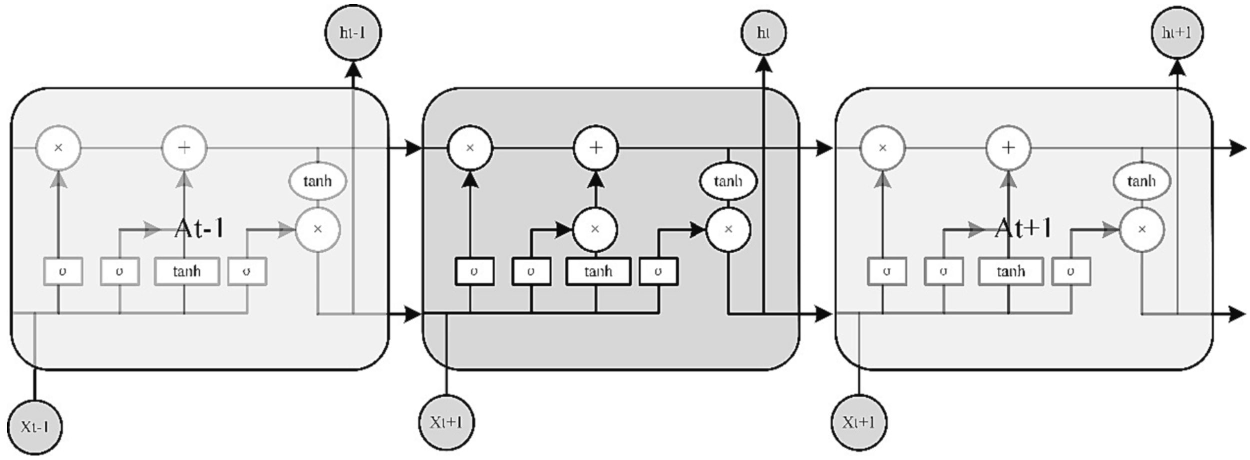

Fig. 1. Structure of the LSTM network.

$$\begin{cases} \Phi(B)\nabla^d x_t = \Theta(B)\varepsilon_t \\ E(\varepsilon_t) = 0, \mathrm{Var}(\varepsilon_t) = \sigma_\varepsilon^2, E(\varepsilon_s\varepsilon_t) = 0, s \neq t \end{cases} \tag{17}$$

$$E(\varepsilon_s\varepsilon_t) = 0, s < t$$

where x_t denotes time series data, x_t is related to $x_{t-i}(i = 1, 2, \cdots, p)$, ε_t denotes the residual term and is related to $\varepsilon_{t-j}(j = 1, 2, \cdots, q)$, B denotes the delay operator, satisfying $B^n x_t = x_{t-n}$, p denotes the autoregressive order, q denotes the moving average order, d denotes the differential order, ∇ denotes the difference operator, $\nabla^d = (1 - B)^d$.

$\Phi(B)$ denotes the autoregressive coefficient polynomial with the following expressions:

$$\Phi(B) = 1 - \phi_1 B - \phi_2 B^2 - \cdots - \phi_p B^p \tag{18}$$

$\Theta(B)$ denotes the moving average coefficient polynomial with the following expressions:

$$\Theta(B) = 1 - \theta_1 B - \theta_2 B^2 - \cdots - \theta_q B^q \tag{19}$$

ε_t is a white noise sequence independent of x_{t-i} and ε_{t-j} that satisfies:

$$\varepsilon_t = \theta_1\varepsilon_{t-1} + \theta_2\varepsilon_{t-2} + \cdots + \theta_q\varepsilon_{t-q} - \phi_0 - \phi_1 x_{t-1} - \phi_2 x_{t-2} - \cdots - \phi_p x_{t-p} - x_t \tag{20}$$

The model satisfying equation (17) is ARIMA (p, d, q), the summation autoregressive sliding average model, which is an organic combination of ARMA (p, q) model and difference operation with high prediction accuracy and low structural requirements for data. For further information, see (Joo & Kim, 2015).

2.5. Long short-term memory (LSTM)

LSTM, proposed by Hochreiter et al (Hochreiter & Schmidhuber, 1997), is a model for processing time series in deep learning. LSTM has solved the long-term dependency problem by improving the chain module structure based on recurrent neural networks (RNN), and is vastly applied in time series forecasting.

The basic unit of LSTM consists mainly of a memory cell and three sets of elemental multiplication gates with adaptive properties, namely input gate, output gate and forget gate. The structure of the memory cell is shown in Fig. 1. For further information, see (Mejia, Avelar-Sosa, Mederos, Ramírez, & Díaz Roman, 2021).

The LSTM model can be expressed as follows with memory cells and gate units.

$$\begin{aligned} f_t &= \sigma\left(W_f x_t + U_f h_{t-1} + b_f\right) \\ i_t &= \sigma(W_i x_t + U_i h_{t-1} + b_i) \\ o_t &= \sigma(W_o x_t + U_o h_{t-1} + b_o) \\ \widetilde{c}_t &= \tanh(W_c x_t + U_c h_{t-1} + b_c) \\ c_t &= f_c{}^\circ c_{t-1} + i_t{}^\circ \widetilde{c}_{t-1} \end{aligned} \tag{21}$$

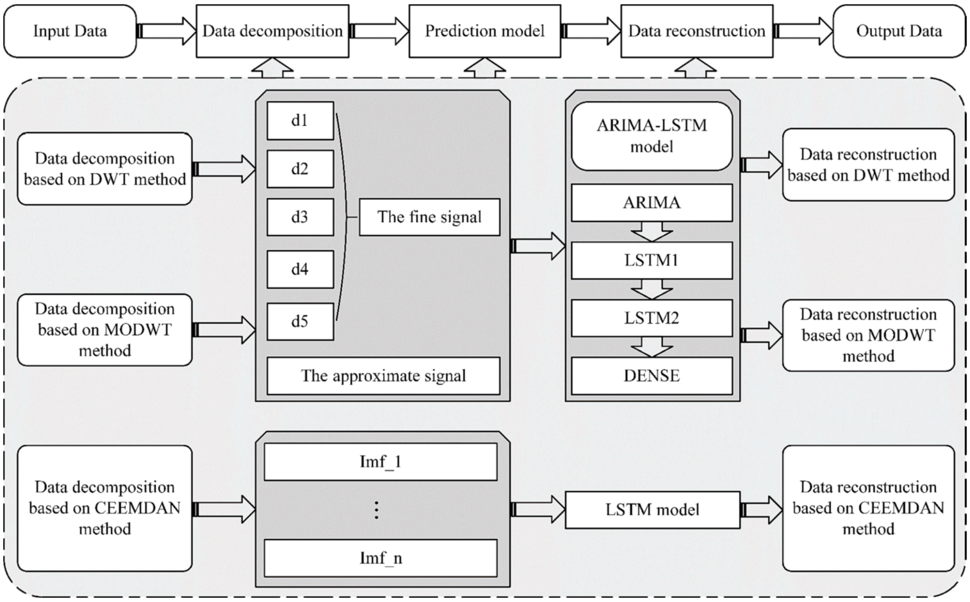

Fig. 2. Structure of hybrid models.

$$h_t = o_t \circ \tanh(c_t)$$

where $x_t \in \mathbb{R}^D$ denotes the input vector at moment t, containing D features. f_t, i_t, o_t, $\widetilde{c}_t$, c_t, h_t denote the forget gate, input gate, output gate, cell input, cell state, and hidden state vectors, respectively. W denotes the weight matrix, b denotes the bias matrix whose value is determined by the training result, $\sigma(\bullet)$ denotes the activation function, generally the sigmoid function, $\circ$ denotes the element-wise product.

2.6. Hybrid model

In this study, a new hybrid model, namely the WT-LSTM-ARIMA, is proposed. The time series is first decomposed using wavelet transform, then the low-frequency and high-frequency decomposed sequences are modelled by ARIMA-LSTM respectively, and finally the low-frequency and high-frequency forecasting are reconstructed to obtain the forecasting. In addition, CEEMDAN-LSTM and MODWT-ARIMA-LSTM models are constructed in this paper as a comparison. The framework of these hybrid models is illustrated in Fig. 2.

The framework is composed of four modules:(1) Wavelet Transform for data processing. It can effectively solve the problems of modal aliasing and residual auxiliary noise and can decompose the unstable stock index sequence into a series of characteristic modal functions. (2) ARIMA for linear relationships processing and time series fitting. We use ARIMA to make rolling forecasts of the stock index futures $c = [c_1, c_2, \cdots c_n]$ and obtain the forecasting sequence $A = [A_1, A_2, \cdots A_n]$. (3) LSTM for non-linear relationships processing and residual sequence fitting. We differentiate the original series from the ARIMA forecasting series to obtain the residual sequence. The residual sequence can be written as follows:

Table 1
Descriptive statistics of the share price index futures.

Furtures	Num	Mean	Std	Skew	Kurt	Min	Q1	Mid	Q3	Max
FDAX	1772	12558.590	1661.950	0.180	−0.460	8476.000	11468.120	12538.500	13411.250	16264.000
NQ	2369	7485.590	3798.230	0.760	−0.650	2701.500	4349.250	6561.500	10783.250	16588.250
YM	2402	23526.570	6476.220	0.370	−1.120	13772.000	17593.250	23545.000	28023.750	36665.000
IF	3092	3461.820	852.310	0.360	−0.640	2055.400	2724.400	3398.000	3981.600	5801.000
IC	1881	6102.160	971.530	1.220	5.140	4033.200	5546.200	6186.600	6488.800	11427.800
IH	1881	2769.900	431.440	0.280	−0.550	1809.800	2415.000	2751.600	3069.600	4020.400
HSIF	2431	24665.970	3175.300	0.020	−0.370	14637.000	22548.000	24366.000	27176.000	33125.000
NK	2386	20969.830	4653.270	0.200	−0.850	11150.000	17125.000	20647.500	23548.750	30485.000
SGP	1480	344.340	33.950	−0.460	−0.670	253.100	321.090	355.100	366.210	412.800
IN	1481	12651.920	3044.560	0.590	−1.040	7547.000	10451.500	11494.500	15709.000	18975.500

Note: Mean denotes the average value, Std denotes standard deviation, Skew denotes skewness, Kurt denotes kurtosis, Min denotes the minimum value, Q1 denotes the first quartile, Mid denotes the median, Q3 denotes the third quartile and Max denotes the maximum value.

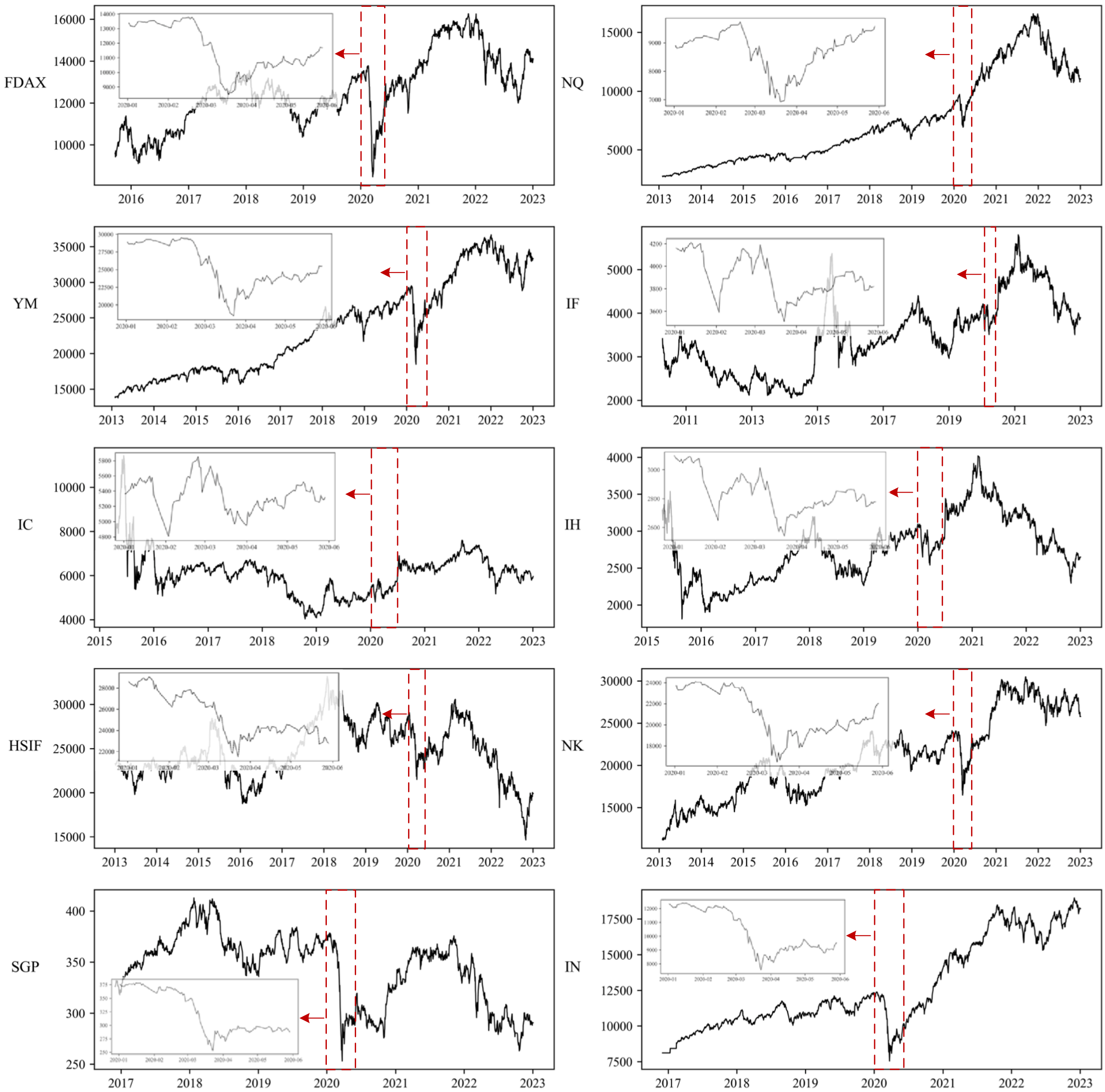

Fig. 3. Time series for daily share price index futures. Note: The red dashed boxes mark data after January 2020. The specific trend from January to June 2020 is shown in the small window on the left. (For interpretation of the references to colour in this figure legend, the reader is referred to the web version of this article.)

$$\Delta A = \Delta A_1, \Delta A_2, \cdots, \Delta A_n, \Delta A_i = c_i - A_i, i = 1, 2, 3\cdots, n \tag{22}$$

The LSTM then is used to learn and predict the residual sequence as following:

$$\Delta E_t = f(\Delta A_{t-1}, \Delta A_{t-2}, \cdots, \Delta A_{t-n}, \cdots) + \varepsilon_t \tag{23}$$

where $f(\bullet)$ represents the non-linear modelling of the LSTM and ε_t is the random error.

Finally, we performs an integrated operation on each feature forecasting output of the LSTM to obtain the final forecasting value as following:

$$P_{LA,t} = A_t + \Delta E_t \tag{24}$$

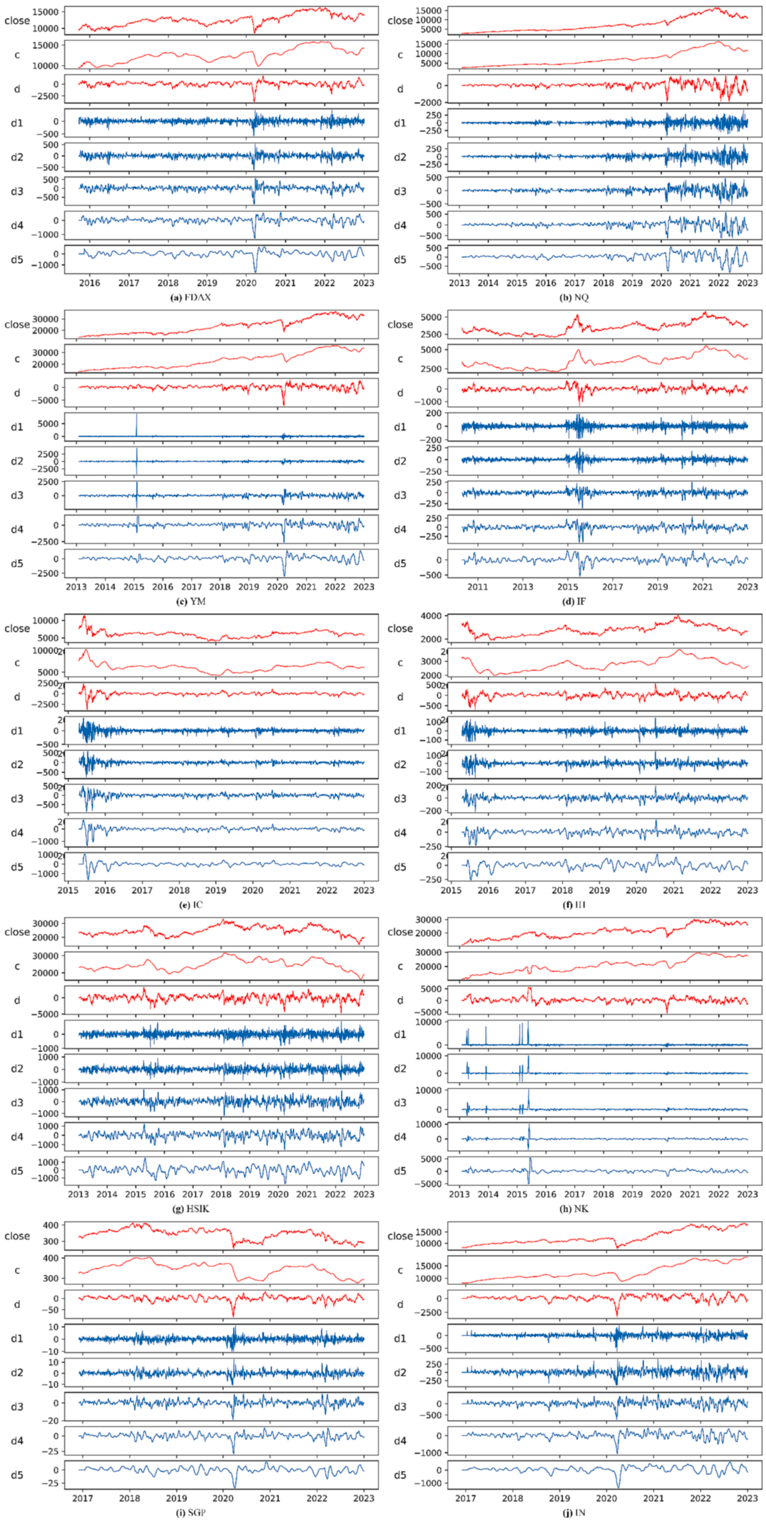

Fig. 4. Decomposed sequences by the DWT method. Note: The red curves close are the original sequence of closing prices; the red curves c are the approximate signals; the blue curves d1-d5 are the fine signals; the red curves d are the synthetic signals of d1-d5. (For interpretation of the references to colour in this figure legend, the reader is referred to the web version of this article.)

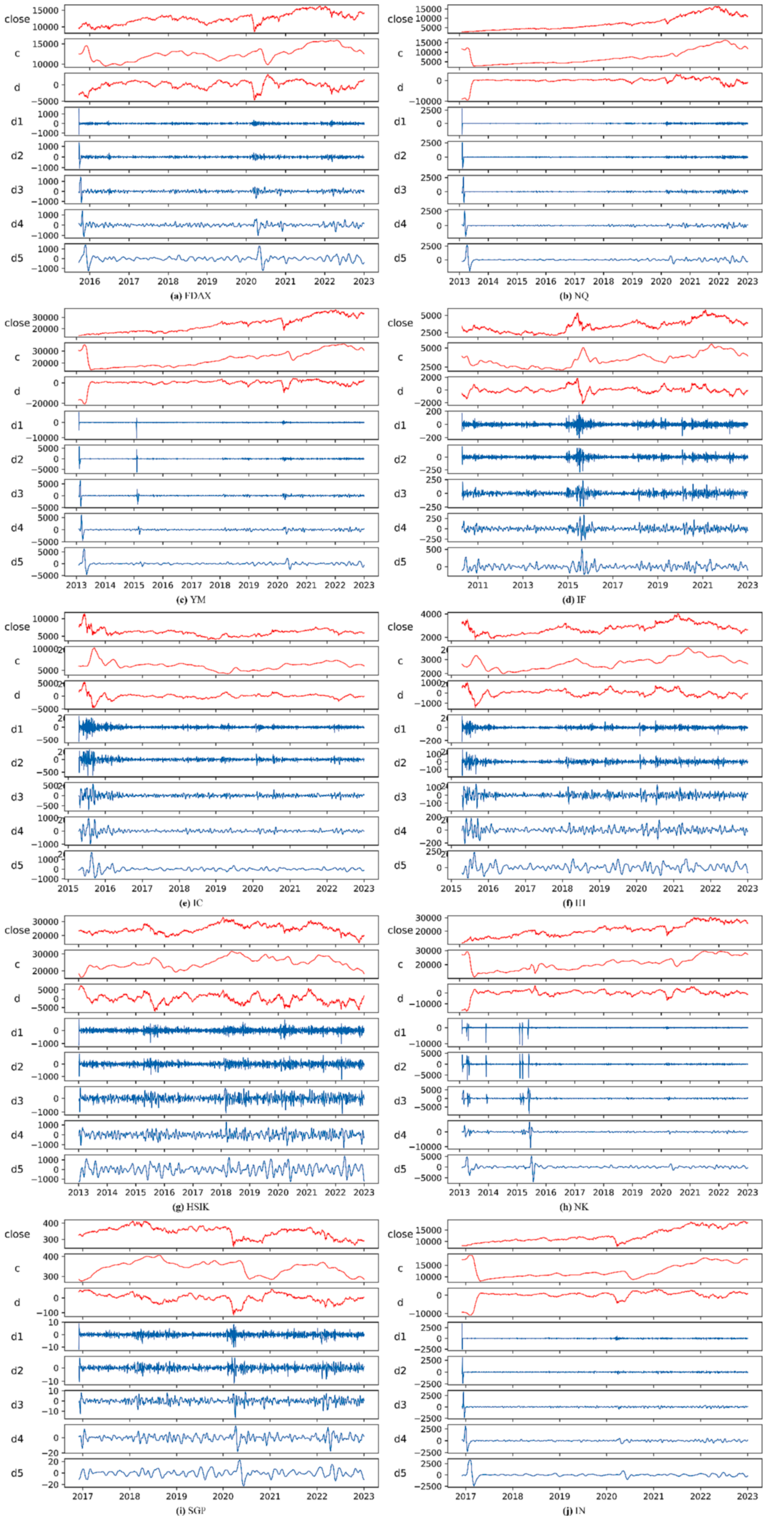

Fig. 5. Decomposed sequences by the MODWT method. Note: The red curves close are the original sequence of closing prices; the red curves c are the approximate signals; the blue curves d1-d5 are the fine signals; the red curves d are the synthetic signals of d1-d5. (For interpretation of the references to colour in this figure legend, the reader is referred to the web version of this article.)

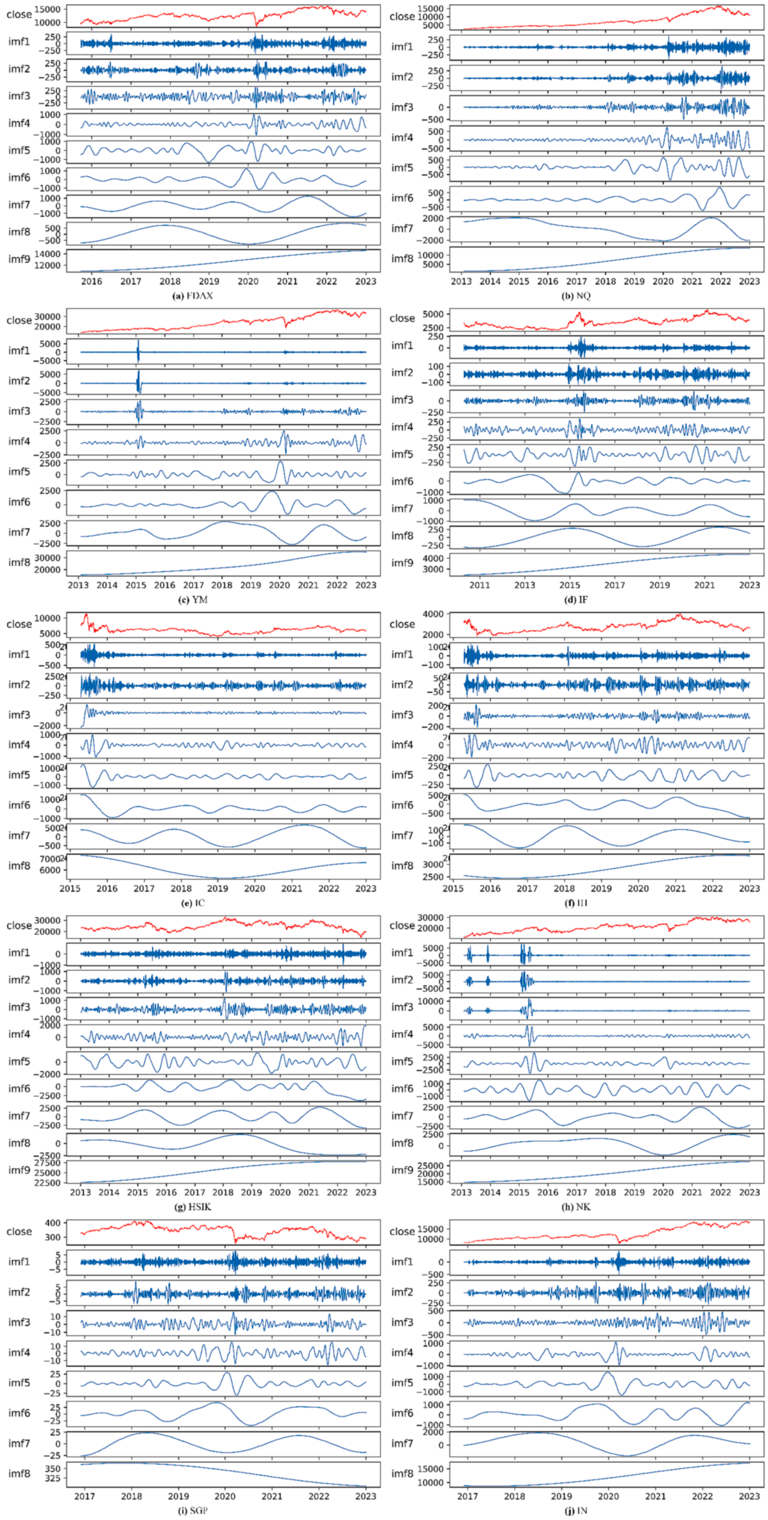

Fig. 6. Decomposed sequences by the CEEMDAN method. Note: The red curves close are the original sequence of closing prices while the blue curves imfi are the decomposed signals. (For interpretation of the references to colour in this figure legend, the reader is referred to the web version of this article.)

Table 2
Signal sequence decomposed by WT.

Futures	DWT	Pearson	Proportion of variance	|Skew|	|Kurt|	MODWT	Pearson	Proportion of variance	|Skew|	|Kurt|
(a) FDAX	c	0.955	0.965	0.246	0.501	c	0.705	0.948	0.255	0.487
	d	0.207	0.088	2.117	11.865	d	0.413	0.575	0.834	0.826
	d1	0.038	0.002	0.515	5.552	d1	−0.001	0.002	2.565	104.450
	d2	0.062	0.003	0.731	4.801	d2	0.001	0.003	1.719	52.672
	d3	0.096	0.006	1.183	7.078	d3	0.000	0.006	0.542	26.890
	d4	0.146	0.012	1.750	9.229	d4	−0.025	0.013	0.085	11.966
	d5	0.214	0.024	2.024	10.884	d5	−0.022	0.027	0.209	7.814
	Average	0.246	0.157	1.224	7.130	Average	0.153	0.225	0.887	29.301
(b) NQ	c	0.995	0.998	0.776	0.639	c	0.895	0.989	0.776	0.643
	d	0.057	0.009	1.259	5.070	d	0.241	0.209	3.576	15.576
	d1	0.012	0.000	0.446	7.541	d1	−0.001	0.001	7.223	481.777
	d2	0.018	0.000	0.430	5.569	d2	0.001	0.001	6.340	284.345
	d3	0.026	0.001	0.712	4.828	d3	0.004	0.001	3.831	135.240
	d4	0.037	0.001	0.949	4.105	d4	−0.004	0.003	2.338	65.524
	d5	0.061	0.002	1.231	4.589	d5	0.004	0.006	2.015	32.971
	Average	0.172	0.145	0.829	4.620	Average	0.163	0.173	3.728	145.154
(c) YM	c	0.992	0.992	0.373	1.108	c	0.851	0.981	0.381	1.103
	d	0.097	0.016	2.482	16.707	d	0.289	0.296	3.865	17.352
	d1	−0.002	0.001	24.904	983.608	d1	0.007	0.002	13.393	678.620
	d2	0.016	0.001	3.614	193.211	d2	−0.001	0.002	0.356	242.378
	d3	0.041	0.002	0.219	23.741	d3	0.001	0.003	2.992	121.367
	d4	0.068	0.002	1.491	10.185	d4	−0.008	0.005	2.426	65.041
	d5	0.104	0.004	2.085	12.953	d5	−0.027	0.011	1.871	33.271
	Average	0.188	0.145	5.024	177.359	Average	0.159	0.186	3.612	165.590
(d) IF	c	0.979	0.978	0.355	0.674	c	0.842	0.984	0.348	0.669
	d	0.158	0.043	0.419	5.219	d	0.295	0.313	0.015	2.536
	d1	0.034	0.001	0.496	8.690	d1	−0.001	0.001	0.234	9.308
	d2	0.054	0.002	0.740	9.795	d2	0.004	0.001	0.517	11.673
	d3	0.078	0.003	0.755	6.791	d3	−0.002	0.002	0.090	4.484
	d4	0.113	0.006	0.939	7.274	d4	−0.003	0.004	0.485	5.236
	d5	0.158	0.011	0.522	5.012	d5	−0.025	0.008	1.039	4.923
	Average	0.225	0.149	0.604	6.208	Average	0.159	0.188	0.390	5.547
(e) IC	c	0.905	0.942	0.878	2.773	c	0.451	0.910	0.899	3.253
	d	0.283	0.185	1.689	14.838	d	0.556	1.050	0.517	8.292
	d1	0.061	0.004	0.902	11.650	d1	0.003	0.004	0.528	16.031
	d2	0.101	0.007	1.232	16.239	d2	0.025	0.005	1.089	17.752
	d3	0.146	0.012	2.005	15.517	d3	−0.037	0.009	0.353	10.947
	d4	0.224	0.027	2.631	21.065	d4	−0.040	0.023	0.360	14.734
	d5	0.248	0.051	1.908	16.077	d5	−0.090	0.049	2.352	20.522
	Average	0.281	0.175	1.606	14.023	Average	0.124	0.293	0.871	13.076
(f) IH	c	0.962	0.967	0.251	0.662	c	0.733	0.966	0.275	0.605
	d	0.197	0.075	0.607	3.107	d	0.386	0.525	0.388	1.864
	d1	0.047	0.003	0.233	7.248	d1	−0.005	0.002	0.716	14.361
	d2	0.072	0.004	0.619	6.333	d2	0.001	0.003	0.643	9.662
	d3	0.104	0.006	0.557	5.182	d3	−0.013	0.005	0.199	4.063
	d4	0.135	0.011	0.823	4.466	d4	0.023	0.010	0.210	3.731
	d5	0.185	0.019	0.662	1.942	d5	−0.072	0.014	0.400	1.554
	Average	0.243	0.155	0.536	4.134	Average	0.150	0.218	0.405	5.120
(g) HSIF	c	0.956	0.937	0.033	0.457	c	0.707	0.964	0.028	0.456
	d	0.253	0.086	0.476	1.222	d	0.404	0.576	0.034	0.028
	d1	0.054	0.003	0.207	3.406	d1	−0.003	0.002	0.431	5.475
	d2	0.086	0.004	0.089	2.388	d2	0.001	0.003	0.539	3.748
	d3	0.126	0.006	0.299	1.318	d3	−0.003	0.005	0.357	1.694
	d4	0.176	0.012	0.503	1.113	d4	−0.021	0.009	0.162	0.969
	d5	0.251	0.022	0.370	0.657	d5	0.000	0.018	0.064	0.357
	Average	0.272	0.153	0.282	1.509	Average	0.155	0.225	0.231	1.818
(h) NK	c	0.978	1.034	0.187	0.866	c	0.783	1.008	0.232	0.886
	d	0.027	0.045	1.011	8.205	d	0.324	0.436	2.953	12.809
	d1	−0.035	0.009	17.616	351.791	d1	0.018	0.012	12.875	274.132
	d2	−0.022	0.009	8.900	181.667	d2	−0.003	0.011	3.971	97.286
	d3	0.004	0.011	8.215	141.482	d3	0.003	0.017	3.561	79.830
	d4	0.025	0.016	5.888	110.316	d4	−0.007	0.026	3.585	77.429
	d5	0.056	0.018	0.561	31.040	d5	−0.021	0.028	0.960	26.256
	Average	0.148	0.163	6.054	117.910	Average	0.157	0.220	4.019	81.232
(i) SGP	c	0.942	0.917	0.455	0.735	c	0.625	0.950	0.430	0.795
	d	0.292	0.113	1.750	7.813	d	0.457	0.732	0.750	1.064
	d1	0.060	0.003	0.048	4.593	d1	−0.003	0.002	0.522	6.509
	d2	0.096	0.004	0.127	3.505	d2	0.008	0.003	0.613	4.228

(*continued on next page*)

Table 2 (*continued*)

Futures	DWT	Pearson	Proportion of variance	|Skew|	|Kurt|	MODWT	Pearson	Proportion of variance	|Skew|	|Kurt|
	d3	0.150	0.008	0.802	5.039	d3	−0.013	0.006	0.784	4.197
	d4	0.217	0.016	1.327	6.819	d4	0.003	0.014	0.446	2.955
	d5	0.275	0.031	1.606	6.469	d5	0.008	0.026	0.077	2.258
	Average	0.290	0.156	0.874	4.996	Average	0.155	0.247	0.517	3.144
(j) IN	c	0.942	0.917	0.455	0.735	c	0.675	0.963	0.635	1.010
	d	0.292	0.113	1.750	7.813	d	0.423	0.639	2.810	8.754
	d1	0.060	0.003	0.048	4.593	d1	−0.001	0.002	7.348	428.739
	d2	0.096	0.004	0.127	3.505	d2	0.001	0.003	6.273	241.353
	d3	0.150	0.008	0.802	5.039	d3	0.006	0.005	4.218	119.037
	d4	0.217	0.016	1.327	6.819	d4	−0.011	0.009	2.429	53.275
	d5	0.275	0.031	1.606	6.469	d5	−0.032	0.020	1.846	25.094
	Average	0.290	0.156	0.874	4.996	Average	0.152	0.234	3.651	125.323

Note: The Pearson coefficients statistically correlate the decomposed series with the original series. The Proportion of variance statistic shows the share of the variance of the decomposed series in the variance of the original series. The results for skewness and kurtosis in the table are absolute. Therefore, larger values of skewness and kurtosis indicate a greater deviation from the normal distribution. C is the approximate signal, D1-D5 is the detail signal and Average is the average of the decomposed series.

3. Empirical analysis

3.1. Data and the descriptive statistics

Ten major share price index futures were selected from several markets for this work, including DAX 30 Index futures (FDAX), NASDAQ 100 Index futures (NQ), Dow Jones Indexes futures (YM), CSI 300 Index futures (IF), CSI 500 Index futures (IC), SSE 50 Index futures (IH), Hang Seng Index futures (HSIF), Nikkei 225 Stock Index futures (NK), MSCI Singapore Index futures (SGP) and Nifty 50 Stock Index futures (IN). The trading data, which includes opening price, closing price, high price, low price and trading volume, are sourced from the Wind database and CSMAR database. The closing price sequence is used as the predicted object, while other trading data (such as opening price, high price, low price, and so on) are used as feature inputs for model training and technical indicator construction. All data are as of December 2022. The start time of different sample data varies due to the different release dates of some indices, with the German DAX starting on September 22, 2015, NQ on February 1, 2013, YM on February 1, 2013, IF on April 16, 2010, IC and IH on April 16, 2015, HSIF on January 4, 2013, NK on February 1, 2013, SGP began on December 1, 2016, and IN began on December 1, 2016. In addition, some of the missing data in the original data were censored.

Table 1 shows the descriptive statistics of the closing prices of the stock index futures after the sample excludes the null values. In addition to the SGP, there is a large difference between the maximum and minimum values of the closing price series of share price index futures. Meanwhile, the NQ is more volatile than the other futures, as shown by the standard deviation statistics. Furthermore, according to the skewness statistics, only the SGP sequence has a negative skewness distribution while the other share price index futures have a positive skewness distribution. The kurtosis statistics show that only IC is high-peak and fat-tailed.

The daily time series for the share price index futures are shown in Fig. 3. It can be seen that the closing prices of the ten futures have gone through different market phases such as up, down, oscillating and reversing during the sample period, thus effectively avoiding the possibility of the forecasting model results being caused by a single trend market.

The outbreak of the COVID-19 in early 2020 has had a knock-on effect on the stability of financial assets and even the linkages between different markets on a global scale. Therefore, the closing price trend at the beginning of the outbreak (after January 2020) is marked by the red dashed box in Fig. 3, and the specific trend during this period is shown in the small chart on the left. It is obvious that at the beginning of the outbreak, the closing price series of futures all show some degree of downward trend, followed by a gradual increase. Changes in the data structure can affect the model's predictive performance, so we discuss the impact of the epidemic shock on the data structure and the model's predictive performance in more detail in the following sections.

All models employed in the following empirical section were implemented using Python 3.6. Among them, the methods related to the wavelet decomposition algorithm are implemented by our code, the CEEMDAN model is implemented using the CEEMDAN package in PyEMD, the ARIMA model is implemented using the auto_arima package in pmdarima and the LSTM model is implemented using the Tensorflow package. The average time per run for the CEEMDAN model was 16.265 s, the average time per run for the DWT model was 0.00283 s, the average time per run for the MODWT model was 0.224 s, the average time per run for the ARIMA model was 12.890 min and the average time per run for the LSTM model was 3.977 min.

3.2. Data decomposition by DWT, MODWT and CEEMDAN methods

The results of the decomposition of the share price index futures are shown in Figs. 4-6. According to signal analysis theory, the approximate signal reflects the low-frequency part of the original series and usually indicates the long-term trend of the original series while the fine signal reflects the high-frequency part of the original series and usually indicates the short-term fluctuation of the original series. It illustrates that the high-frequency sequences have greater volatility and contain more noise; the low-frequency sequence is relatively stable and represents the underlying trend of stock prices. For comparison with the other two methods, the results of the direct wavelet decomposition are shown here, while the first-order differencing was performed in the subsequent

Table 3
Signal sequence decomposed by CEEMDAN.

Futures		Pearson	Variance	$\lvert$Skew$\rvert$	$\lvert$Kurt$\rvert$	Futures		Pearson	Variance	$\lvert$Skew$\rvert$	$\lvert$Kurt$\rvert$
(a) FDAX	imf1	0.039	0.002	0.155	2.060	(f) IH	imf1	0.047	0.003	0.152	4.691
	imf2	0.052	0.002	0.059	1.984		imf2	0.040	0.003	0.036	1.029
	imf3	0.108	0.005	0.028	0.490		imf3	0.065	0.007	0.066	6.048
	imf4	0.098	0.019	0.203	3.674		imf4	0.081	0.015	0.132	0.938
	imf5	0.235	0.056	0.785	1.853		imf5	0.105	0.054	0.210	0.716
	imf6	0.102	0.064	0.021	0.640		imf6	0.477	0.375	0.251	0.070
	imf7	0.433	0.155	0.030	0.560		imf7	0.455	0.059	0.012	1.227
	imf8	0.523	0.119	0.125	1.469		imf8	0.683	0.656	0.244	1.559
	imf9	0.739	0.538	0.130	1.426		Average	0.244	0.147	0.138	2.035
	Average	0.259	0.107	0.171	1.573	(g) HSIF	imf1	0.041	0.003	0.062	2.044
(b) NQ	imf1	0.020	0.000	0.009	4.995		imf2	0.104	0.004	0.107	3.500
	imf2	0.059	0.000	0.198	5.916		imf3	0.111	0.007	0.145	1.718
	imf3	0.047	0.001	0.022	5.470		imf4	0.088	0.023	0.380	1.785
	imf4	0.025	0.002	0.020	4.149		imf5	0.221	0.048	0.130	0.168
	imf5	0.062	0.005	0.193	2.071		imf6	0.597	0.166	0.951	0.677
	imf6	0.156	0.004	0.094	3.566		imf7	0.702	0.230	0.001	0.951
	imf7	−0.266	0.143	0.311	1.303		imf8	0.402	0.180	0.032	1.207
	imf8	0.941	1.326	0.125	1.486		imf9	0.295	0.333	0.289	1.446
	Average	0.130	0.185	0.121	3.619		Average	0.284	0.110	0.233	1.500
(c) YM	imf1	0.016	0.003	0.428	195.814	(h) NK	imf1	0.031	0.026	0.594	45.910
	imf2	0.023	0.006	0.285	94.165		imf2	−0.016	0.032	0.597	32.880
	imf3	0.008	0.003	0.410	23.285		imf3	−0.013	0.058	2.855	50.559
	imf4	0.093	0.005	0.919	6.910		imf4	0.023	0.026	2.024	24.809
	imf5	0.049	0.010	0.560	4.281		imf5	0.115	0.033	0.563	6.547
	imf6	0.072	0.012	0.858	2.696		imf6	0.162	0.017	0.054	0.146
	imf7	0.129	0.054	0.067	0.942		imf7	0.074	0.075	0.280	0.271
	imf8	0.960	0.974	0.533	1.101		imf8	0.328	0.073	0.458	0.841
	Average	0.169	0.133	0.508	41.149		imf9	0.915	0.857	0.194	1.400
(d) IF	imf1	0.037	0.001	0.043	9.528		Average	0.180	0.133	0.847	18.152
	imf2	0.045	0.001	0.009	1.782	(i) SGP	imf1	0.052	0.003	0.094	1.484
	imf3	0.021	0.003	0.254	3.225		imf2	0.075	0.003	0.146	1.905
	imf4	0.080	0.009	0.093	1.595		imf3	0.136	0.012	0.328	1.420
	imf5	0.152	0.022	0.078	0.174		imf4	0.115	0.023	0.015	0.653
	imf6	0.186	0.154	1.085	2.276		imf5	0.169	0.058	0.274	3.131
	imf7	0.327	0.368	0.140	0.766		imf6	0.512	0.359	0.281	0.403
	imf8	0.366	0.069	0.081	1.522		imf7	0.529	0.189	0.005	1.384
	imf9	0.781	0.588	0.072	1.466		imf8	0.606	0.400	0.400	1.379
	Average	0.222	0.135	0.206	2.482		Average	0.274	0.131	0.193	1.470
(e) IC	imf1	0.094	0.005	0.293	13.346	(j) IN	imf1	0.035	0.001	0.011	4.348
	imf2	0.075	0.004	0.069	2.892		imf2	0.048	0.001	0.098	1.490
	imf3	−0.050	0.075	4.796	39.466		imf3	0.048	0.002	0.067	2.780
	imf4	0.181	0.045	0.720	6.819		imf4	0.056	0.006	0.220	3.904
	imf5	0.312	0.109	0.349	6.784		imf5	0.124	0.021	0.321	2.935
	imf6	0.502	0.175	0.805	2.987		imf6	0.122	0.035	0.076	0.696
	imf7	0.550	0.160	0.014	1.255		imf7	0.191	0.118	0.640	0.705
	imf8	0.672	0.412	0.263	1.114		imf8	0.911	0.946	0.329	1.403
	Average	0.292	0.123	0.914	9.333		Average	0.192	0.141	0.220	2.283

Note: The Pearson coefficients statistically correlate the decomposed series with the original series. The Proportion of variance statistic shows the share of the variance of the decomposed series in the variance of the original series. The results for skewness and kurtosis in the table are absolute. Therefore, larger values of skewness and kurtosis indicate a greater deviation from the normal distribution. Imfi is the decomposition component i.

building of the ARIMA model.

Both the DWT and MODWT methods can effectively decompose the closing price series. Figs. 4 and 5 show that the detailed signals obtained from the decomposition of the MODWT method have more robust boundary effects and less volatility, but the approximate signals are more volatile than the results of the DWT method and can't characterize the long-term trend. The CEEMDAN method can effectively filter the noise of the original sequence and solve the problem of transferring the transmission of the sequence from high to low frequencies. Meanwhile, a clear trend can be seen in the low-frequency sequences.

The statistical characteristics of the wavelet decomposition series are presented in Table 2 and the statistical characteristics of the decomposition components of the CEEMDAN method are presented in Table 3, where the skewness and kurtosis are presented in absolute values. The average Pearson correlation coefficients of the wavelet decomposition series of the share price index futures are all lower, indicating that the wavelet decomposed series contain less noise and can better extract data characteristics of different frequencies. Similarly, the skewness of the decomposed series is closer to 0, indicating that the symmetry of the data is better, and the kurtosis of the decomposed series is greater than 3, indicating that the data presents the characteristics of high-peak and fat-tail.

First, compared to the DWT method and the CEEMDAN method, the decomposition sequence correlation of the MODWT method is

Table 4
Statistics of stationarity test.

(A) DWT		ADF test			KPSS test		
		(a) close	(b) c	(c) d	(d) close	(e) c	(f) d
FDAX	Original sequence	−2.226	−1.587	−8.150***	3.934***	3.908***	0.048
	First order differential	−16.939***	−6.951***	−11.169***	0.040	0.063	0.006
NQ	Original sequence	−1.005	−0.813	−9.452***	7.109***	7.115***	0.159
	First order differential	−12.456***	−8.846***	−12.920***	0.110	0.173	0.007
YM	Original sequence	−0.960	−0.514	−9.757***	7.608***	7.627***	0.033
	First order differential	−12.991***	−10.208***	−11.920***	0.024	0.043	0.005
IF	Original sequence	−1.833	−1.191	−8.104***	6.189***	6.231***	0.066
	First order differential	−10.999***	−11.377***	−14.261***	0.064	0.090	0.003
IC	Original sequence	−3.973***	−3.412**	−8.299***	1.001***	1.124***	0.120
	First order differential	−10.767***	−9.987***	−12.937***	0.044	0.099	0.005
IH	Original sequence	−1.779	−1.917	−6.726***	3.345***	3.291***	0.193
	First order differential	−8.834***	−7.366***	−11.232***	0.112	0.236	0.005
HSIF	Original sequence	−2.145	−2.746*	−7.404***	1.225***	1.263***	0.169
	First order differential	−51.217***	−7.830***	−13.353***	0.092	0.210	0.005
NK	Original sequence	−1.954	−1.448	−8.476***	6.874***	7.034***	0.310
	First order differential	−12.806***	−10.646***	−12.310***	0.057	0.045	0.009
SGP	Original sequence	−1.777	−1.138	−7.594***	2.217***	2.102***	0.173
	First order differential	−25.887***	−6.323***	−11.364***	0.106	0.205	0.006
IN	Original sequence	−0.645	−0.424	−6.502***	4.742***	4.746***	0.104
	First order differential	−15.143***	−6.669***	−15.408***	0.071	0.126	0.010
(B) MODWT		ADF test			KPSS test		
		(a) close	(b) c	(c) d	(d) close	(e) c	(f) d
FDAX	Original sequence	−2.226	−1.417	−4.130***	3.934***	3.174***	0.277
	First order differential	−16.939***	−8.619***	−13.546***	0.040	0.073	0.052
NQ	Original sequence	−1.005	−1.449	−5.576***	7.109***	5.896***	0.829***
	First order differential	−12.456***	−7.523***	−9.153***	0.110	0.444*	0.388*
YM	Original sequence	−0.960	−1.615	−5.668***	7.608***	5.980***	0.799***
	First order differential	−12.991***	−8.846***	−9.292***	0.024	0.244	0.185
IF	Original sequence	−1.833	−1.609	−5.876***	6.189***	5.798***	0.217
	First order differential	−10.999***	−7.144***	−9.462***	0.064	0.122	0.020
IC	Original sequence	−3.973***	−2.219	−6.233***	1.001***	1.009***	0.087
	First order differential	−10.767***	−6.903***	−8.548***	0.044	0.036	0.030
IH	Original sequence	−1.779	−1.246	−5.839***	3.345***	3.849***	0.246
	First order differential	−8.834***	−8.815***	−7.176***	0.112	0.098	0.048
HSIF	Original sequence	−2.145	−1.992	−5.084***	1.225***	2.160***	0.807***
	First order differential	−51.217***	−7.223***	–22.913***	0.092	0.346	0.053
NK	Original sequence	−1.954	−1.639	−6.224***	6.874***	5.506***	0.408*
	First order differential	−12.806***	−11.026***	−9.542***	0.057	0.192	0.251
SGP	Original sequence	−1.777	−1.373	−3.188**	2.217***	0.993***	0.799***
	First order differential	−25.887***	−7.486***	−14.762***	0.106	0.397*	0.050
IN	Original sequence	−0.645	−1.617	−4.936***	4.742***	2.658***	0.967***
	First order differential	−15.143***	−7.804***	−6.0***	0.071	0.337	0.232

Note: Column (a) and (d) are the results of the original closing price series stationarity test, column (b) and (e) are the results of the approximate signal series stationarity test, column (c) and (f) are the results of the detailed signal series stationarity test. In the ADF test, Critical Value (1%): −3.433; Critical Value (5%): −2.863; Critical Value (10%): −2.567. In the KPSS test, Critical Value (1%): 0.739; Critical Value (5%): 0.463; Critical Value (10%): 0.347.

Table 5
The statistics of significance tests.

5–1 Low frequency series						
	Coefficient	Standard error	z	$P > \|z\|$	[0.025	0.975]
Constants	2.8978	0.202	14.316	0.000	2.501	3.295
ar.L1.D.c5	0.7537	0.065	11.676	0.000	0.627	0.880
5–2 High frequency series						
	Coefficient	Standard error	z	$P > \|z\|$	[0.025	0.975]
Constants	−94.4488	78.567	−1.202	0.229	−248.437	59.539
ar.L1.d	0.9641	0.026	37.617	0.000	0.914	1.014

lower, especially the correlation of the approximate signal is lower. Secondly, in terms of variance share, the average variance share of DWT method is lower and that of the MODWT method is higher, which is due to the higher fluctuation of the fine signal of the MODWT method. Finally, the CEEMDAN method is closer to the normal distribution in the data distribution. Consequently, the statistical results

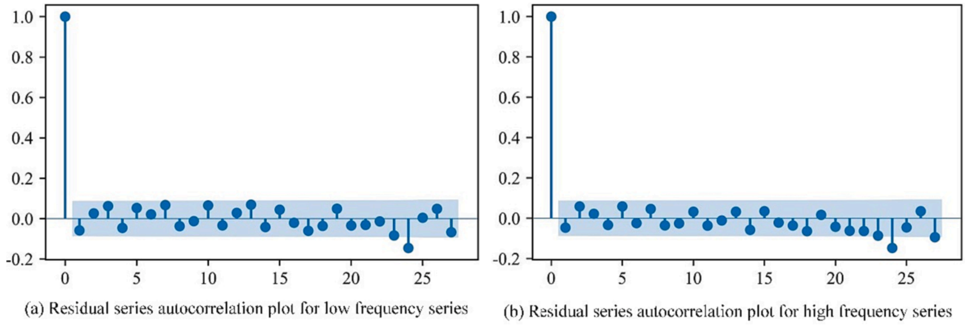

Fig. 7. Residual autocorrelation test. Note: The blue area in the figure shows the confidence interval. (For interpretation of the references to colour in this figure legend, the reader is referred to the web version of this article.)

Table 6
The statistics of the D-W test.

	Low frequency series	How frequency series
D-W statistics	2.040	1.727

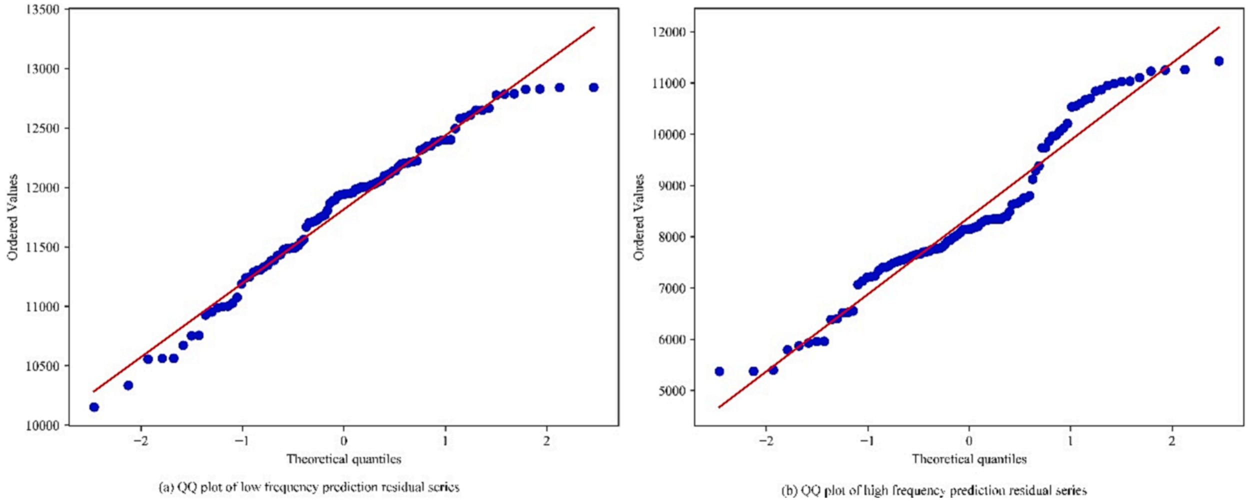

Fig. 8. QQ-plot for forecasting residuals series. Note: The blue scatter points are residuals and the red line is the fitted curve in the figure. (For interpretation of the references to colour in this figure legend, the reader is referred to the web version of this article.)

of the decomposed sequences show the advantages and disadvantages of each of the three methods.

Overall, the MODWT method has a more robust boundary effect compared to the DWT method, namely it can handle signals of any length and is less affected by similar boundaries. However, it sacrifices the performance of the algorithm to filter the signal, so the DWT method has a better denoising capability.

3.3. Implementation of the ARIMA-LSTM model

3.3.1. Stationarity test

Stationarity is tested using the Augmented Dickey-Fuller (ADF) test and the Kwiatkowski-Phillips-Schmidt-Shin (KPSS) test.

(1) The ADF test

The ADF test can be expressed as follows:

$$\Delta X_t = \sigma X_{t-1} + \sum_{i=1}^{m} \beta_i \Delta X_{t-i} + \epsilon_t \tag{25}$$

Table 7
The statistics of the LB test for low frequency series.

Lag	AC	Q	Prob(>Q)	Lag	AC	Q	Prob(>Q)
1	−0.029	0.088	0.766	21	−0.006	14.379	0.853
2	0.109	1.303	0.521	22	−0.046	14.654	0.877
3	0.003	1.304	0.728	23	−0.180	18.907	0.707
4	−0.022	1.355	0.852	24	−0.066	19.482	0.726
5	0.077	1.992	0.850	25	−0.051	19.830	0.756
6	−0.152	4.470	0.613	26	0.022	19.898	0.796
7	0.078	5.139	0.643	27	0.045	20.185	0.823
8	−0.148	7.536	0.480	28	−0.059	20.683	0.838
9	−0.099	8.618	0.473	29	0.018	20.727	0.869
10	−0.112	10.029	0.438	30	0.105	22.318	0.842
11	0.058	10.413	0.494	31	−0.053	22.736	0.859
12	−0.060	10.827	0.544	32	0.065	23.368	0.866
13	0.089	11.755	0.548	33	0.013	23.394	0.892
14	0.071	12.351	0.578	34	0.027	23.505	0.912
15	0.108	13.749	0.545	35	−0.028	23.629	0.928
16	0.044	13.986	0.600	36	−0.146	27.028	0.860
17	0.035	14.139	0.657	37	0.005	27.031	0.886
18	−0.004	14.141	0.720	38	−0.078	28.021	0.882
19	−0.009	14.150	0.775	39	−0.077	29.009	0.879
20	−0.042	14.374	0.811	40	−0.013	29.039	0.900

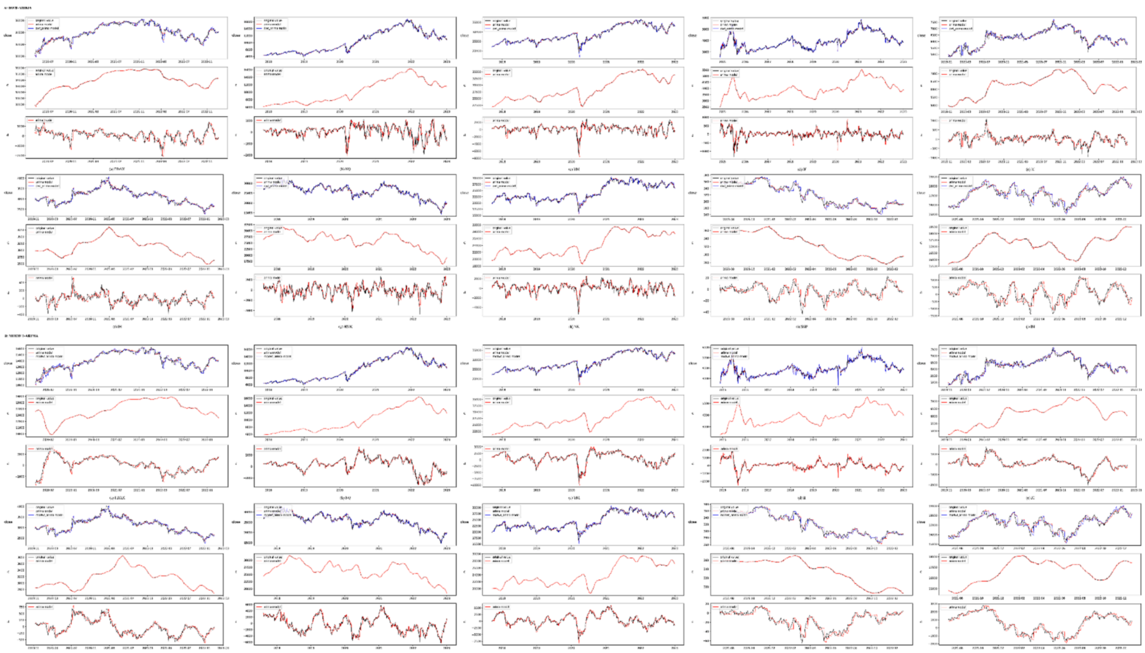

Fig. 9. ARIMA model forecasting. Note: The black line in the chart is the actual series, the red blue line is the ARIMA model forecast result and the blue line is the WT-ARIMA model forecast result. A shows the prediction results of the WT-ARIMA model with the benchmark model while B shows the prediction results of the DWT-ARIMA model with the benchmark model. For each underlying, the prediction results of the model for the closing price series, the approximate signal c series and the detailed signal d series are shown from top to bottom. (For interpretation of the references to colour in this figure legend, the reader is referred to the web version of this article.)

$$\Delta X_t = \alpha + \sigma X_{t-1} + \sum_{i=1}^{m} \beta_i \Delta X_{t-i} + \epsilon_t \tag{26}$$

$$\Delta X_t = \alpha + \beta t + \sigma X_{t-1} + \sum_{i=1}^{m} \beta_i \Delta X_{t-i} + \epsilon_t \tag{27}$$

where, ϵ_t is assumed to have a mean equal to 0 and a standard deviation equal to the random error value of σ; σ is assumed to be constant for any t.

The original and alternative hypotheses for the KPSS test are illustrated as follows.

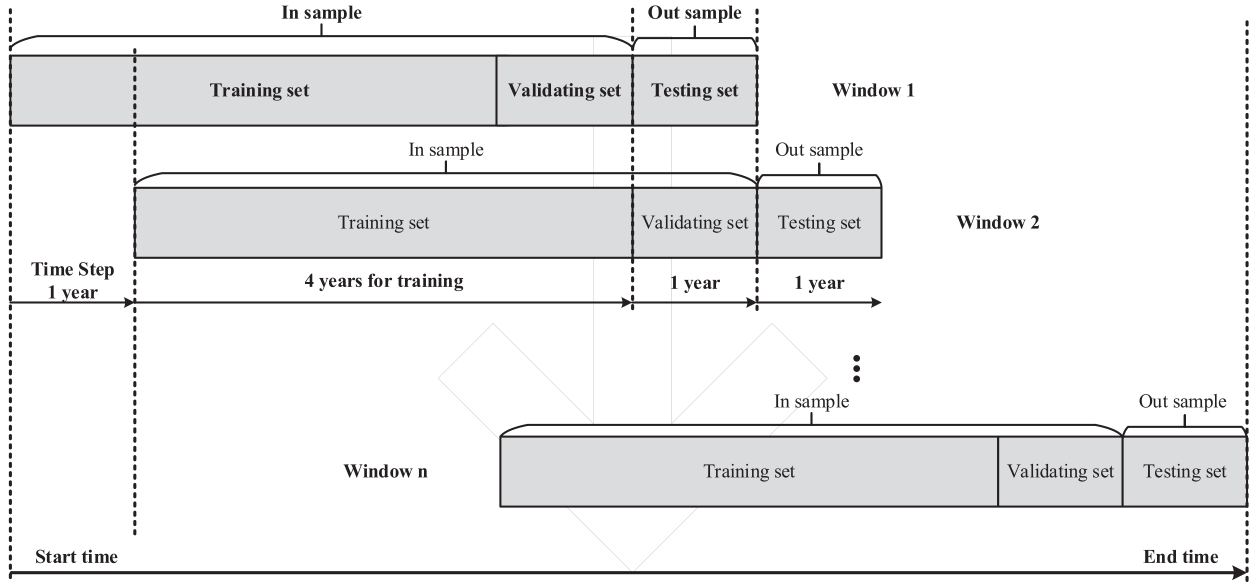

Fig. 10. Distribution of training, validation and test datasets.

Table 8
Technical Analysis Indicator.

Technical Analysis Indicator		Calculation formula
Moving Average Convergence and Divergence (MACD)	The MACD is an indicator for buying and selling from a short-term perspective, using an exponential moving average to smooth the price of a stock.	$\mathrm{DIF_t} = \mathrm{EMA_{short_t}} - \mathrm{EMA_{long_t}}$ $\mathrm{DEA_t} = \mathrm{EMA(DIF_t, period_3)}$ $\mathrm{MACD_t} = 2 \times (\mathrm{DIF_t} - \mathrm{DEA_t})$ where, $\mathrm{EMA_{long_t}} = \mathrm{EMA(closeprice_t, period_1)}$, $\mathrm{EMA_{short_t}} = \mathrm{EMA(closeprice_t, period_2)}$, closeprice indicates the closing price, *period_1*, *period_2*, *period_3* indicates the calculation period, which is less than or equal to the sample length. EMA is an exponential smoothed moving average calculation function.
Relative Strength Index (RSI)	The RSI measures the strength of market movement trends in terms of the relative strength of asset price increases and decreases.	$\mathrm{RSI(n)} = \frac{A}{(A+B)} \times 100\%$ Where, A indicates the increase in price over n days and B indicates the decrease in price over n days. A +B indicates the total volatility over the time period.
On Balance Volume (OBV)	OBV's forecasting of price is based on the observation and analysis of volume.	$\text{Next day OBV} = \text{base period OBV} \pm \text{next day volume}$ $\textit{Net long/short ratio} = \frac{2 \times closeprice - lowprice - highprice}{highprice - lowprice \times Volume}$

The null hypothesis $H_0 : \sigma = 0$, the original series has a unit root and is non-stationary;

Alternative hypothesis $H_1 : \sigma < 0$, the original series has no unit root and is stationary.

(2) The KPSS test

The original and alternative hypotheses of the KPSS test are the opposite of the ADF test. The null hypothesis is that the original series does not have a unit root and is stationary; the alternative hypothesis is that the original series has a unit root and is non–stationary.

The results of the tests are presented in Table 4. Columns (a)-(c) ADF show the statistical values for the ADF test on the original closing price series and the wavelet-decomposed series, namely the approximate signal and the detail signal. Taking FDAX as an example, in column (a), the test statistic for the original series of the closing price series is −2.226, which is greater than the statistical values of −3.43, −2.86 and −2.57 for the rejection of the original hypothesis at the 1 %, 5 % and 10 % levels, thus the null hypothesis cannot be rejected, namely the original series is non-stationary; the p-value of the series after the first-order difference is close to zero and the test statistic is −16.939, so the null hypothesis can be rejected, namely the series after the first-order difference is stationary.

Columns (d)-(f) KPSS show the statistical values for the KPSS test. Taking FDAX as an example, in column (d), the test statistic for the original series of the closing price series is 3.934 greater than the statistical values of 0.739, 0.463 and 0.347 for rejecting the original hypothesis at the 1 %, 5 % and 10 % levels, which rejects the null hypothesis that the original series is non-stationary; the test statistic for the series after first order differencing is 0.04, which accepts the null hypothesis that the series after first-order differencing is stationary.

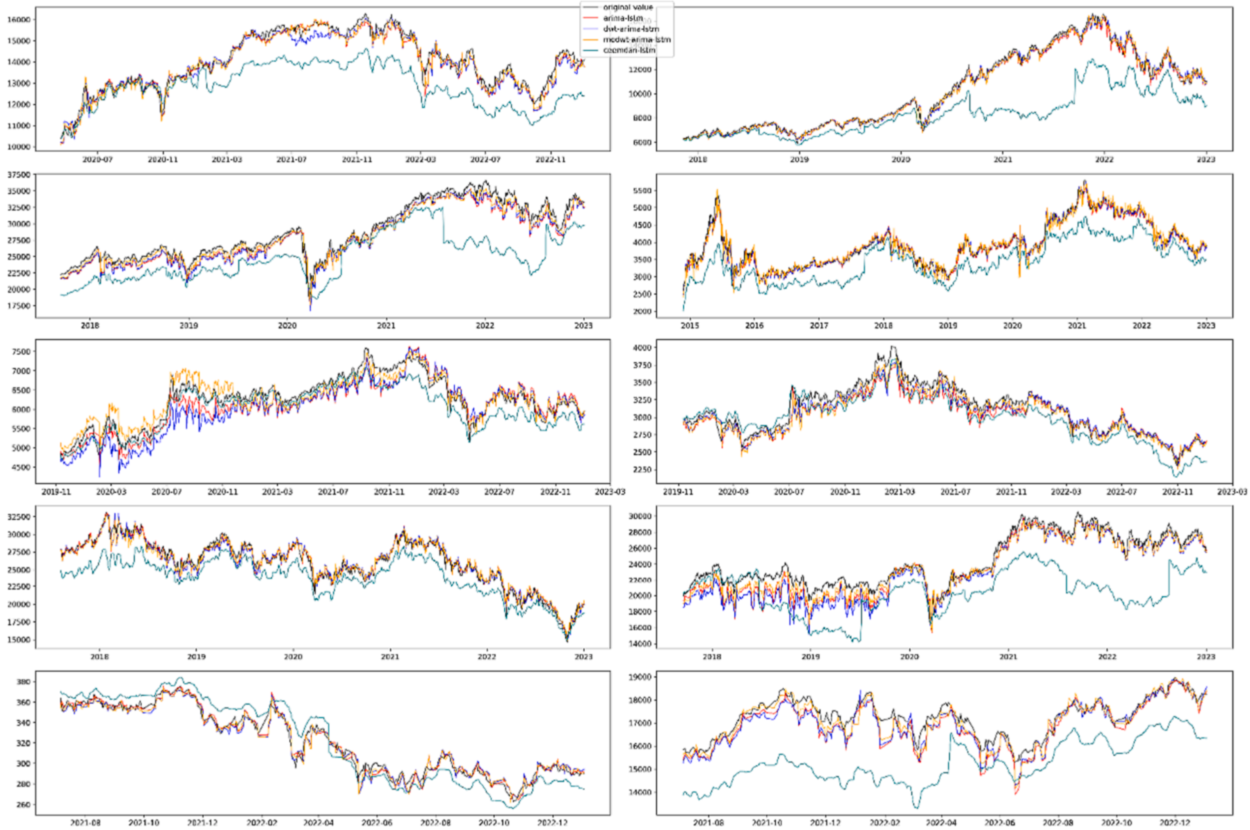

Fig. 11. Forecasting results of hybrid model. Note: The black line in the figure shows the actual series, the red line is the forecast result of the ARIMA-LSTM model, the blue line is the forecast result of the DWT-ARIMA-LSTM model, the yellow line is the forecast result of the MODWT-ARIMA-LSTM model and the green line is the forecast result of the CEEMDAN-LSTM model. From top left to bottom right, the forecasting results of FDAX, NQ, YM, IF, IC, IH, HSIF, NK, SGP and IN closing prices are shown in order. (For interpretation of the references to colour in this figure legend, the reader is referred to the web version of this article.)

3.3.2. *Model identification and parameter estimation*

In this part, a rolling forecast approach is applied to determine the applicable parameters of the ARIMA model, and the model was trained with a time window of 100 days to forecast the next 5 days of data. The BIC criterion is used to determine the order of the model. The first training window data for the IF is shown below as an example.

BIC criterion is vastly applied for model selection, as following:

$$BIC = mln(n) - 2ln(L) \tag{28}$$

where m and L denote the complexity and fitting capability of the model, respectively, and n is the sample size of the model. $mln(n)$ is a penalty term that helps the model control the complexity of its choice of parameters when it is faced with a smaller sample size.

To check the parametric adequacy of the ARIMA, we performed significance tests on the parameters of the model and autocorrelation, normality and randomness tests on the residual series.

(1) Significance test

The statistics of the significance tests of the parameters of the model by z-variables are shown in Table 5. Table 5-1 shows the statistics of the low frequency series test and Table 5-2 shows the statistics of the high frequency series test, with p-values less than 0.05 and 0.10, and the parameters passed the significance tests.

(2) Residual autocorrelation test

The residuals of the fitted series should be non-autocorrelated and the residuals should not contain series generated by the AR or MA process. Therefore, the residuals from the model fit were tested using an autocorrelation plot and the Durbin-Watson test. The autocorrelation plot of the forecast residuals is shown in Fig. 7, and it is clear that the autocorrelation coefficients converge rapidly to within the 95 % confidence interval after order 1.

The D-W test is vastly applied for first-order autocorrelation test. Its original hypothesis is as follows:

H0:$\rho = 0$, which indicates there is no first-order serial correlation of random error terms.

Define the D-W statistic as follows:

Table 9
Predictive accuracy statistics.

		In sample			Out sample		
		MAE	MAPE	RMSE	MAE	MAPE	RMSE
FDAX	DWT-ARIMA-LSTM	**221.838**	**1.629 %**	311.912	**222.194**	**1.640 %**	312.896
	DWT-ARIMA	243.269	1.783 %	330.226	243.317	1.792 %	343.812
	MODWT-ARIMA	237.006	1.809 %	3641.784	247.482	1.833 %	345.129
	DWT-LSTM	410.716	2.857 %	511.932	416.518	2.879 %	523.800
	MODWT-LSTM	589.723	3.985 %	722.126	597.039	4.124 %	707.753
	CEEMDAN-LSTM	927.755	5.928 %	1235.074	994.991	6.846 %	1332.482
	LSTM	1058.036	7.119 %	1239.224	1179.429	8.177 %	1335.366
	ARIMA	234.504	1.680 %	307.275	244.453	1.766 %	314.227
	ARIMA-LSTM	265.958	1.889 %	339.244	275.995	1.980 %	347.042
	MODWT-ARIMA-LSTM	227.756	1.639 %	**294.966**	230.255	1.670 %	**293.975**
NQ	DWT-ARIMA-LSTM	**159.580**	**1.699 %**	**238.172**	**188.314**	**1.839 %**	276.836
	DWT-ARIMA	168.024	1.777 %	256.457	197.395	1.921 %	294.580
	MODWT-ARIMA	167.910	1.788 %	247.854	197.899	1.935 %	285.719
	DWT-LSTM	426.375	3.800 %	599.034	468.696	4.028 %	631.628
	MODWT-LSTM	656.212	5.823 %	885.904	695.496	5.978 %	901.649
	CEEMDAN-LSTM	720.742	6.522 %	929.562	841.062	7.272 %	1041.276
	LSTM	1903.589	15.983 %	2627.930	1971.718	16.255 %	2662.872
	ARIMA	212.272	2.131 %	282.876	229.269	2.172 %	303.602
	ARIMA-LSTM	193.790	2.035 %	257.454	216.858	2.122 %	284.944
	MODWT-ARIMA-LSTM	190.800	1.995 %	256.679	207.048	2.028 %	**272.585**
YM	DWT-ARIMA-LSTM	**398.886**	**1.441 %**	**631.471**	**400.577**	**1.446 %**	**636.377**
	DWT-ARIMA	417.716	1.515 %	656.115	421.487	1.521 %	657.811
	MODWT-ARIMA	429.250	1.488 %	651.930	430.091	1.561 %	653.182
	DWT-LSTM	3132.051	10.505 %	3429.259	3135.142	10.791 %	3443.950
	MODWT-LSTM	2310.974	7.605 %	2620.073	2328.514	7.847 %	2635.067
	CEEMDAN-LSTM	2706.102	9.044 %	3205.630	2787.773	9.198 %	3387.665
	LSTM	3875.581	13.133 %	4547.670	3876.633	13.198 %	4554.995
	ARIMA	1023.472	3.609 %	1190.646	1031.485	3.611 %	1200.473
	ARIMA-LSTM	977.154	3.239 %	1113.744	988.683	3.499 %	1155.317
	MODWT-ARIMA-LSTM	732.584	2.325 %	910.212	746.456	2.599 %	913.860
IF	DWT-ARIMA-LSTM	**78.323**	**2.008 %**	119.652	**78.874**	**2.031 %**	122.017
	DWT-ARIMA	83.263	2.134 %	125.866	83.735	2.156 %	128.123
	MODWT-ARIMA	102.432	2.624 %	154.693	103.572	2.668 %	156.851
	DWT-LSTM	134.744	3.241 %	169.581	137.549	3.301 %	174.621
	MODWT-LSTM	206.690	5.040 %	240.825	213.487	5.201 %	249.065
	CEEMDAN-LSTM	244.923	6.029 %	281.296	252.899	6.230 %	290.689
	LSTM	491.925	12.389 %	538.702	511.719	12.912 %	558.761
	ARIMA	81.662	2.095 %	114.251	83.763	2.160 %	117.582
	ARIMA-LSTM	77.373	1.998 %	**110.018**	79.313	2.058 %	**113.377**
	MODWT-ARIMA-LSTM	95.769	2.449 %	131.684	97.415	2.501 %	134.655
IC	DWT-ARIMA-LSTM	**106.237**	**1.736 %**	**147.036**	**106.980**	**1.749 %**	**147.581**
	DWT-ARIMA	111.143	1.813 %	154.378	112.051	1.829 %	155.055
	MODWT-ARIMA	113.510	1.855 %	157.062	114.195	1.868 %	157.235
	DWT-LSTM	410.233	6.758 %	540.524	411.534	6.781 %	541.032
	MODWT-LSTM	547.955	9.000 %	703.123	551.271	9.021 %	708.494
	CEEMDAN-LSTM	434.477	6.223 %	451.777	400.342	6.458 %	456.916
	LSTM	240.579	3.791 %	293.041	241.755	3.815 %	293.612
	ARIMA	222.008	3.423 %	270.013	240.202	3.796 %	278.525
	ARIMA-LSTM	300.065	4.712 %	353.445	300.503	4.872 %	356.359
	MODWT-ARIMA-LSTM	184.462	3.011 %	223.395	186.152	3.031 %	227.313
IH	DWT-ARIMA-LSTM	**52.962**	**1.713 %**	**74.896**	**53.135**	**1.716 %**	**75.179**
	DWT-ARIMA	54.702	1.764 %	76.555	54.728	1.767 %	76.599
	MODWT-ARIMA	57.203	1.850 %	77.501	57.367	1.852 %	77.800
	DWT-LSTM	88.692	2.736 %	109.050	89.323	2.752 %	109.643
	MODWT-LSTM	129.205	4.013 %	150.470	130.095	4.034 %	151.277
	CEEMDAN-LSTM	207.800	6.541 %	225.544	209.699	6.595 %	226.903
	LSTM	164.104	5.288 %	177.969	165.480	5.353 %	179.478
	ARIMA	104.433	3.213 %	133.871	105.488	3.243 %	134.709
	ARIMA-LSTM	79.654	2.480 %	104.026	80.366	2.500 %	104.658
	MODWT-ARIMA-LSTM	79.741	2.506 %	102.764	80.465	2.527 %	103.381
HSIF	DWT-ARIMA-LSTM	**466.507**	**1.808 %**	**624.215**	**471.174**	**1.871 %**	628.302
	DWT-ARIMA	492.809	1.905 %	666.145	497.640	1.971 %	669.778
	MODWT-ARIMA	497.131	1.929 %	665.458	501.615	1.993 %	669.243
	DWT-LSTM	621.385	2.376 %	789.719	627.348	2.399 %	796.362
	MODWT-LSTM	710.054	2.662 %	898.536	713.407	2.701 %	904.561
	CEEMDAN-LSTM	827.190	3.122 %	1081.559	835.439	3.151 %	1092.958
	LSTM	2158.972	8.144 %	2393.340	2223.096	8.326 %	2439.904

(*continued on next page*)

Table 9 (*continued*)

		In sample			Out sample		
		MAE	MAPE	RMSE	MAE	MAPE	RMSE
	ARIMA	469.470	1.850 %	602.334	472.119	**1.871 %**	**604.884**
	ARIMA-LSTM	528.102	2.071 %	666.898	532.986	2.086 %	671.746
	MODWT-ARIMA-LSTM	475.980	1.848 %	611.115	476.005	1.886 %	612.489
NK	DWT-ARIMA-LSTM	**373.533**	**1.572 %**	**531.128**	**374.833**	**1.573 %**	**531.489**
	DWT-ARIMA	391.370	1.638 %	542.219	391.698	1.643 %	543.002
	MODWT-ARIMA	407.136	1.712 %	561.906	408.939	1.723 %	564.539
	DWT-LSTM	1807.256	7.298 %	1937.958	1827.547	7.386 %	1953.350
	MODWT-LSTM	2333.067	9.607 %	2546.964	2356.737	9.716 %	2566.520
	CEEMDAN-LSTM	2436.776	9.785 %	2692.552	2453.812	9.865 %	2709.288
	LSTM	4007.979	15.960 %	4682.826	4016.966	16.017 %	4702.175
	ARIMA	1006.257	4.344 %	1274.154	1018.412	4.402 %	1284.622
	ARIMA-LSTM	1368.494	5.948 %	1699.157	1387.837	6.038 %	1714.651
	MODWT-ARIMA-LSTM	874.265	3.730 %	1051.318	885.140	3.780 %	1060.195
SGP	DWT-ARIMA-LSTM	**2.994**	**0.990 %**	**3.498**	**4.110**	**1.298 %**	**5.410**
	DWT-ARIMA	4.712	1.543 %	6.650	5.203	1.644 %	7.242
	MODWT-ARIMA	4.298	1.408 %	5.974	4.766	1.505 %	6.543
	DWT-LSTM	5.292	1.680 %	7.006	6.634	2.029 %	8.180
	MODWT-LSTM	6.995	2.234 %	8.599	8.096	2.476 %	9.765
	CEEMDAN-LSTM	8.467	2.709 %	9.745	9.707	2.973 %	10.872
	LSTM	10.961	3.309 %	12.274	11.255	3.557 %	12.317
	ARIMA	4.108	1.357 %	5.310	4.340	1.382 %	5.704
	ARIMA-LSTM	4.306	1.415 %	5.519	4.603	1.455 %	5.909
	MODWT-ARIMA-LSTM	4.360	1.327 %	5.806	4.775	1.512 %	6.754
IN	DWT-ARIMA-LSTM	**221.151**	**1.277 %**	**286.795**	**232.510**	**1.363 %**	**306.491**
	DWT-ARIMA	225.084	1.301 %	301.253	242.176	1.420 %	322.982
	MODWT-ARIMA	234.035	1.350 %	301.875	242.293	1.418 %	317.078
	DWT-LSTM	716.800	4.118 %	820.160	881.101	5.129 %	952.072
	MODWT-LSTM	1203.951	6.920 %	1343.054	1428.187	8.331 %	1544.061
	CEEMDAN-LSTM	962.547	5.538 %	1032.073	1053.556	6.162 %	1129.933
	LSTM	1722.102	9.847 %	1859.684	1967.369	11.389 %	2097.876
	ARIMA	290.627	1.687 %	400.151	375.159	2.203 %	476.018
	ARIMA-LSTM	279.074	1.619 %	382.276	370.019	2.169 %	457.318
	MODWT-ARIMA-LSTM	232.443	1.348 %	313.773	276.976	1.630 %	363.852

Note: The range of values of mean absolute error (MAE), which calculated as MAE $=\frac{1}{m}\sum_{i=1}^{m}|y_i-\hat{y}_i|$, is $[0,+\infty]$. This indicator is zero when the predicted and actual values are exactly the same, and the greater the error, the greater the value of the indicator. The range of values of mean absolute percentage error (MAPE), which calculated as MAPE $=\frac{100\%}{m}\sum_{i=1}^{m}\left|\frac{y_i-\hat{y}_i}{y_i}\right|$, is $[0,+\infty]$. This indicator is 0 % when the predicted and actual values are exactly the same, while when the indicator is greater than 100 %, it indicates poor model quality. The range of values of root mean square error (RMSE), which calculated as RMSE $=\sqrt{\frac{1}{m}\sum_{i=1}^{m}(y_i-\hat{y}_i)^2}$, is $[0,+\infty]$. The indicator is zero if the predicted and actual values are identical, while the larger the error, the larger the value of the indicator. The bolded values indicate the lowest prediction error.

$$D = 2(1-\rho) \tag{29}$$

When the DW value is significantly closer to 0 or 4 then there is autocorrelation and closer to 2 then there is no (first order) autocorrelation. Thus, at a given level of significance, we can test the original hypothesis H0 depending on the critical value.

$$\begin{cases} D\rightarrow 2, \rho\rightarrow 0 \\ D\rightarrow 0, \rho\rightarrow 1 \\ D\rightarrow 4, \rho\rightarrow -1 \end{cases} \tag{30}$$

The statistics of the D-W test performed on the fitted residuals of this paper are shown in Table 6. The DW statistic is close to 2, so the autocorrelation coefficient ρ is close to 0 and the residual series can be considered to have no first-order autocorrelation.

(3) Residual normality test

The residuals of the model should be normally distributed, and the QQ plot, shown in Fig. 8, visualizes the distribution of the residual series. It can be seen that the overall dispersion is around the diagonal, namely the residual series follows a normal distribution.

(4) Residual randomness test

The residuals of the ARIMA model fitted series should be Gaussian white noise, so, in this study, the Ljung-Box test is applied to perform randomness or lagged correlation tests on the residuals. The following is an example of the low frequency series, and the statistics are shown in Table 7. According to the statistics, the p-values are greater than the significance level at all orders of lag, the original hypothesis cannot be rejected and the series is white noise.

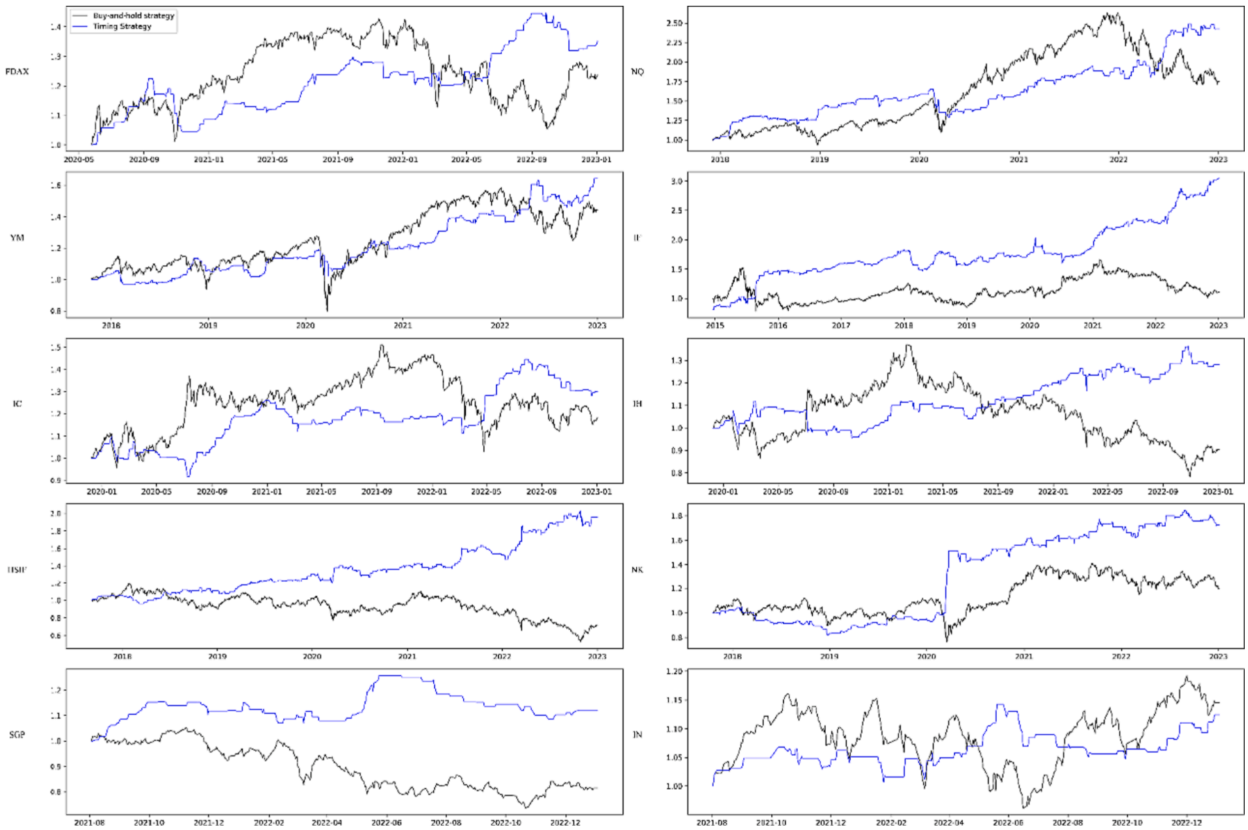

Fig. 12. Net curves for strategies. Note: The black curve is the net curve of the timing strategy and the blue curve is the net curve of the buy-and-hold strategy. The vertical axis shows the net value of the strategy. (For interpretation of the references to colour in this figure legend, the reader is referred to the web version of this article.)

Table 10
Strategy back-testing statistics.

Futures	Strategy	Annualised return	Annualised volatility	Sharpe ratio	Maximum retracement
FDAX	Buy-and-hold strategy	10.461 %	19.957 %	0.374	26.224 %
	Timing trading strategy	**12.514 %**	**10.564 %**	**0.901**	**14.519 %**
NQ	Buy-and-hold strategy	14.769 %	25.650 %	0.459	35.325 %
	Timing trading strategy	**19.188 %**	**14.705 %**	**1.101**	**21.897 %**
YM	Buy-and-hold strategy	9.511 %	21.134 %	0.308	37.403 %
	Timing trading strategy	**10.606 %**	**12.070 %**	**0.630**	**14.194 %**
IF	Buy-and-hold strategy	4.876 %	26.444 %	0.071	48.717 %
	Timing trading strategy	**18.329 %**	**15.064 %**	**1.018**	**21.483 %**
IC	Buy-and-hold strategy	8.236 %	22.142 %	0.236	31.931 %
	Timing trading strategy	**9.704 %**	**12.838 %**	**0.522**	**16.552 %**
IH	Buy-and-hold strategy	−0.997 %	22.211 %	−0.180	42.931 %
	Timing trading strategy	**9.330 %**	**13.744 %**	**0.461**	**14.684 %**
HSIF	Buy-and-hold strategy	−3.687 %	23.565 %	−0.284	55.813 %
	Timing trading strategy	**13.884 %**	**12.660 %**	**0.860**	**10.083 %**
NK	Buy-and-hold strategy	5.833 %	21.320 %	0.133	31.942 %
	Timing trading strategy	**11.682 %**	**12.921 %**	**0.672**	**21.818 %**
SGP	Buy-and-hold strategy	−13.258 %	19.174 %	−0.848	30.007 %
	Timing trading strategy	**8.971 %**	**10.206 %**	**0.585**	**13.715 %**
IN	Buy-and-hold strategy	**11.190 %**	16.069 %	0.510	17.183 %
	Timing trading strategy	9.056 %	**9.619 %**	**0.630**	**8.371 %**

Note: Annualised return is calculated as $Ret = (P_t/P_0)/T \times 252$; annualised volatility is calculated as $\sigma = \sigma_{SD}/\sqrt{1/252}$; Sharpe ratio is calculated as $Sharpe = (Ret - rf)/\sigma$; maximum retracement is calculated as $MaxDown = \max\left[(P_i - P_j)/P_i\right]$. The bolded values indicate best strategy performance.

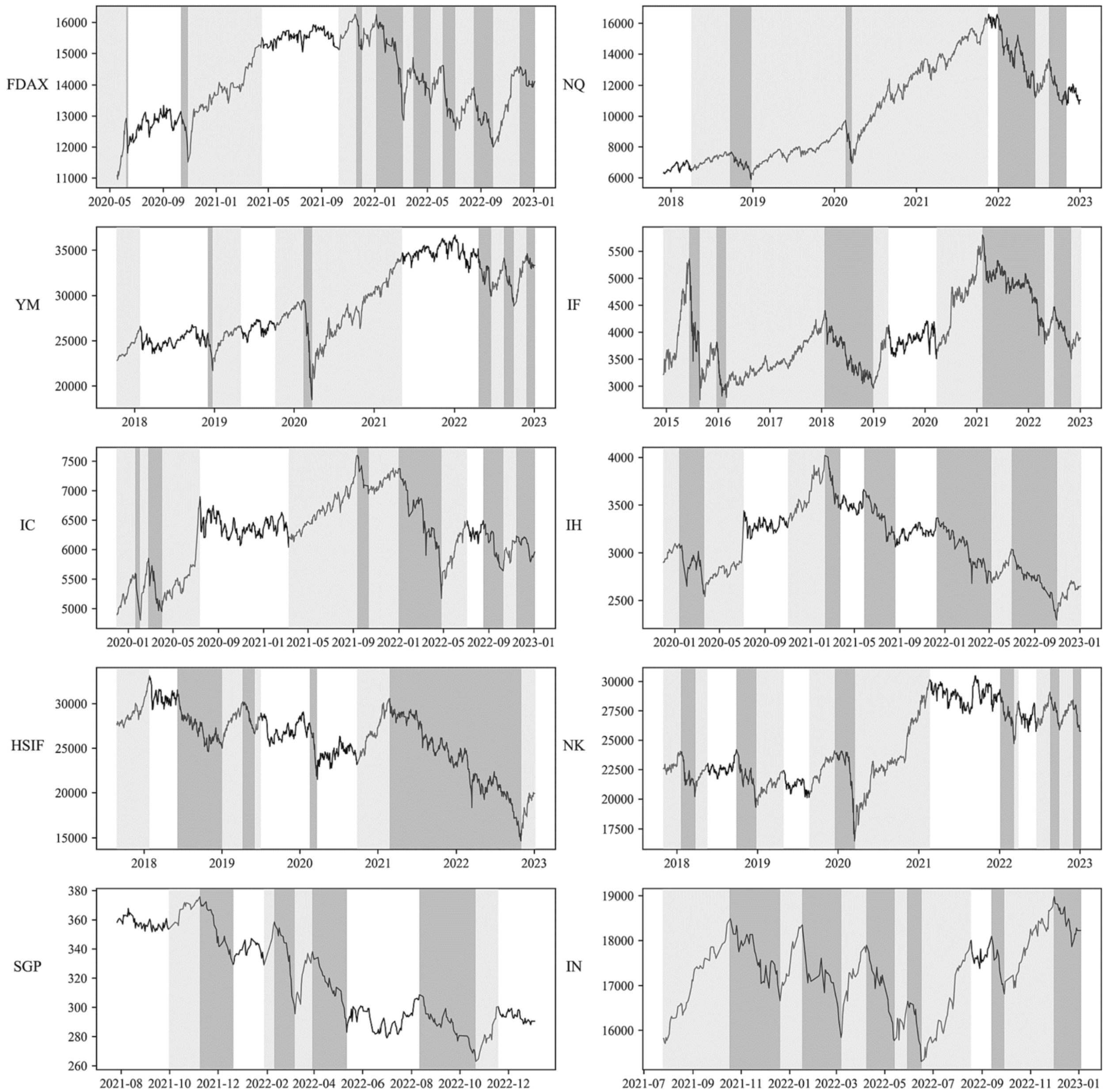

Fig. 13. Division of three different market quotation periods. Note: The upside periods are indicated by a light gray box. The downside periods are indicated by a dark gray box and the oscillation periods are represented in white.

Combined with the above test results, the model parameters were set reasonably.

3.3.3. ARIMA model forecasting results

The prediction results of the ARIMA model for the selected futures returns are shown in Fig. 9. The predicted values of the ARIMA model, the predicted values of the WT-ARIMA models, the ARIMA models and the actual values are represented by blue lines, red lines and black lines, respectively. The predicted results of the DWT-ARIMA models are shown in Fig. 9-A and the predicted results of the MODWT-ARIMA models are shown in Fig. 9-B. According to Fig. 9, it can be concluded that the model using the WT method achieves better forecasting results for different share price index futures in different markets.

3.3.4. Implementation of the LSTM model

A forward rolling window is used for model training. We selected data from the last 4 years as the training set for model training, and the data from the last 1 year as the validation set to adjust the model; finally, the trained model was applied to predict data from the last 1 year. The distribution of training, validation, and test datasets is shown in Fig. 10. In each time window (5 years), the

Table 11
Strategy back-testing statistics of three different market quotation periods.

Futures	Period	Strategy	Annualised return	Annualised volatility	Sharpe ratio	Maximum retracement
FDAX	upside period	Timing trading	**32.089 %**	**20.059 %**	**1.301**	**7.999 %**
		Buy-and-hold	30.428 %	34.426 %	0.797	26.224 %
	downside period	Timing trading	26.315 %	**25.966 %**	**0.898**	**8.769 %**
		Buy-and-hold	**26.982 %**	61.034 %	0.393	25.505 %
	oscillation period	Timing trading	**31.059 %**	**11.311 %**	**2.392**	**9.233 %**
		Buy-and-hold	30.257 %	25.402 %	1.073	6.131 %
NQ	upside period	Timing trading	20.137 %	**16.963 %**	**1.010**	**20.852 %**
		Buy-and-hold	**27.510 %**	32.448 %	0.755	30.606 %
	downside period	Timing trading	77.195 %	**53.676 %**	**1.382**	**18.150 %**
		Buy-and-hold	**102.056 %**	146.330 %	0.677	33.263 %
	oscillation period	Timing trading	**209.188 %**	120.733 %	**1.708**	**2.706 %**
		Buy-and-hold	137.928 %	**99.713 %**	1.353	10.713 %
YM	upside period	Timing trading	17.075 %	**13.534 %**	**1.040**	**10.760 %**
		Buy-and-hold	**17.513 %**	27.926 %	0.520	29.339 %
	downside period	Timing trading	**109.644 %**	**47.928 %**	**2.225**	**14.194 %**
		Buy-and-hold	79.468 %	127.434 %	0.837	37.403 %
	oscillation period	Timing trading	25.396 %	**15.993 %**	**1.400**	**5.336 %**
		Buy-and-hold	**28.826 %**	33.948 %	0.761	11.286 %
IF	upside period	Timing trading	**34.008 %**	**22.152 %**	**1.400**	**13.448 %**
		Buy-and-hold	11.426 %	38.800 %	0.217	47.727 %
	downside period	Timing trading	**43.823 %**	**33.269 %**	**1.227**	**18.493 %**
		Buy-and-hold	3.577 %	67.952 %	0.009	48.717 %
	oscillation period	Timing trading	**11.431 %**	**15.110 %**	**0.558**	**11.256 %**
		Buy-and-hold	−9.424 %	23.043 %	−0.539	14.886 %
IC	upside period	Timing trading	22.190 %	**20.217 %**	**0.949**	**14.657 %**
		Buy-and-hold	**22.256 %**	34.118 %	0.564	29.941 %
	downside period	Timing trading	**27.087 %**	**33.326 %**	**0.723**	**10.313 %**
		Buy-and-hold	24.696 %	60.340 %	0.360	30.009 %
	oscillation period	Timing trading	**53.367 %**	25.430 %	**1.981**	11.070 %
		Buy-and-hold	−3.269 %	**20.424 %**	−0.307	**10.432 %**
IH	upside period	Timing trading	**28.125 %**	**20.067 %**	**1.252**	**10.400 %**
		Buy-and-hold	10.118 %	42.398 %	0.168	32.201 %
	downside period	Timing trading	**20.736 %**	**17.001 %**	**1.043**	**9.592 %**
		Buy-and-hold	−10.771 %	46.537 %	−0.296	39.540 %
	oscillation period	Timing trading	**36.766 %**	21.479 %	**1.572**	**5.058 %**
		Buy-and-hold	−0.701 %	**20.493 %**	−0.181	8.632 %
HSIF	upside period	Timing trading	**48.786 %**	**35.258 %**	**1.299**	**8.731 %**
		Buy-and-hold	−4.026 %	50.735 %	−0.138	54.753 %
	downside period	Timing trading	**28.964 %**	**18.982 %**	**1.368**	**10.083 %**
		Buy-and-hold	−26.297 %	36.969 %	−0.792	51.248 %
	oscillation period	Timing trading	**21.080 %**	**15.823 %**	**1.143**	**9.067 %**
		Buy-and-hold	−18.965 %	28.374 %	−0.774	35.106 %
NK	upside period	Timing trading	**30.250 %**	34.343 %	**0.793**	**18.669 %**
		Buy-and-hold	17.021 %	**31.254 %**	0.449	28.411 %
	downside period	Timing trading	**54.548 %**	**35.598 %**	**1.448**	**21.818 %**
		Buy-and-hold	31.282 %	80.683 %	0.351	31.942 %
	oscillation period	Timing trading	**47.641 %**	46.188 %	**0.966**	**5.394 %**
		Buy-and-hold	14.533 %	**36.159 %**	0.319	15.631 %
SGP	upside period	Timing trading	**2.312 %**	**13.524 %**	**−0.051**	**7.416 %**
		Buy-and-hold	−35.905 %	43.409 %	−0.896	27.771 %
	downside period	Timing trading	**−2.133 %**	**13.180 %**	**−0.389**	**8.783 %**
		Buy-and-hold	−63.300 %	23.670 %	−2.801	28.318 %
	oscillation period	Timing trading	**25.660 %**	**18.244 %**	**1.242**	**11.067 %**
		Buy-and-hold	−40.084 %	23.232 %	−1.854	24.109 %
IN	upside period	Timing trading	14.123 %	**14.028 %**	0.793	**7.223 %**
		Buy-and-hold	**22.664 %**	21.708 %	**0.906**	14.436 %
	downside period	Timing trading	**11.114 %**	**13.953 %**	**0.582**	**8.371 %**
		Buy-and-hold	4.380 %	28.439 %	0.049	17.183 %
	oscillation period	Timing trading	−5.446 %	**4.892 %**	−1.726	**1.629 %**
		Buy-and-hold	**−1.239 %**	15.147 %	**−0.280**	3.463 %

Note: The bolded values indicate best strategy performance.

prediction results of the first 4 years (training set) are in-sample predictions, and the prediction results of the last year (test set) are out-of-sample predictions.

The feature set used in the models includes trading data (closing price decomposition data, opening price, high price, low price and volume), technical indicators (Moving Average Convergence and Divergence, Relative Strength Index and On Balance Volume are

Table 12
KS test.

Futures	KS test	P-value
NQ	0.899	0
YM	0.732	2.03E-172
IF	0.635	2.62E-176
HSIF	0.632	6.66E-16
NK	0.754	7.76E-185

Table 13
Model prediction performance statistics before and after the COVID-19 outbreak.

Futures	Period	MAE	MAPE	RMSE
NQ	Pre-COVID-19	172.945	1.732 %	242.626
	Post-COVID-19	200.097	1.963 %	308.333
YM	Pre-COVID-19	383.653	1.359 %	611.155
	Post-COVID-19	410.675	1.488 %	667.841
IF	Pre-COVID-19	79.443	2.200 %	129.100
	Post-COVID-19	77.835	1.722 %	107.870
HSIF	Pre-COVID-19	449.479	1.598 %	610.466
	Post-COVID-19	490.324	2.112 %	643.635
NK	Pre-COVID-19	397.816	1.651 %	546.910
	Post-COVID-19	360.782	1.475 %	529.587

Table 14
Strategy back-testing statistics of different epidemic phases.

Futures	Period	Strategy	Annualised return	Annualised volatility	Sharpe ratio	Maximum retracement
NQ	Pre-COVID-19	Timing trading	**23.215 %**	**11.492 %**	**1.759**	**8.683 %**
		Buy-and-hold	18.465 %	19.541 %	0.791	23.198 %
	Early Outbreak	Timing trading	**−108.873 %**	**41.700 %**	**−2.683**	**18.150 %**
		Buy-and-hold	−182.755 %	62.442 %	−2.975	28.908 %
	Post-COVID-19	Timing trading	**16.441 %**	**16.751 %**	**0.802**	**21.897 %**
		Buy-and-hold	11.165 %	29.416 %	0.278	35.325 %
YM	Pre-COVID-19	Timing trading	6.329 %	**8.411 %**	0.396	**10.840 %**
		Buy-and-hold	**11.022 %**	15.067 %	**0.532**	18.878 %
	Early Outbreak	Timing trading	**−10.700 %**	**44.502 %**	**−0.308**	**14.194 %**
		Buy-and-hold	−279.011 %	63.851 %	−4.417	36.042 %
	Post-COVID-19	Timing trading	**13.759 %**	**14.329 %**	**0.751**	**14.194 %**
		Buy-and-hold	8.798 %	24.883 %	0.233	37.403 %
IF	Pre-COVID-19	Timing trading	**17.430 %**	**16.171 %**	**0.892**	**19.630 %**
		Buy-and-hold	7.443 %	28.793 %	0.154	48.717 %
	Early Outbreak	Timing trading	−86.200 %	**20.463 %**	−4.359	**11.256 %**
		Buy-and-hold	**11.823 %**	31.838 %	**0.277**	14.500 %
	Post-COVID-19	Timing trading	**14.905 %**	**11.517 %**	**1.034**	**21.483 %**
		Buy-and-hold	5.108 %	21.172 %	0.100	39.572 %
HSIF	Pre-COVID-19	Timing trading	**12.223 %**	**9.290 %**	**0.993**	**9.295 %**
		Buy-and-hold	2.467 %	18.139 %	−0.029	25.769 %
	Early Outbreak	Timing trading	**40.035 %**	**22.791 %**	**1.625**	**5.612 %**
		Buy-and-hold	−88.729 %	34.005 %	−2.698	21.554 %
	Post-COVID-19	Timing trading	**17.825 %**	**14.431 %**	**1.027**	**10.083 %**
		Buy-and-hold	−6.082 %	26.973 %	−0.337	52.140 %
NK	Pre-COVID-19	Timing trading	−2.279 %	**9.012 %**	−0.586	21.818 %
		Buy-and-hold	**5.473 %**	17.479 %	**0.141**	**20.289 %**
	Early Outbreak	Timing trading	**255.341 %**	**43.595 %**	**5.788**	**3.081 %**
		Buy-and-hold	−188.145 %	59.635 %	−3.205	31.332 %
	Post-COVID-19	Timing trading	**21.627 %**	**15.079 %**	**1.235**	**8.627 %**
		Buy-and-hold	7.088 %	23.857 %	0.171	31.332 %

Note: Pre-COVID-19 indicates data prior to January 2020. Post-COVID-19 indicates data after January 2020. Early Outbreak indicates data from January to March 2020. The bolded values indicate best strategy performance.

selected for technical analysis indicators, as shown in Table 8) and macro indicators (RMB exchange rate, SHIBOR, US dollar exchange rate and FFR, data from CSMAR database and Wind database) for 7 days prior to this date. The model structure is chosen as a double-layer LSTM with the following hyperparameters: the learning rate is 10ˆ(-4) and the number of iterations is 300.

Table A1
Futures Code.

Name of futures	Symbol	Market
DAX 30 Index futures	FDAX	Germany
NASDAQ 100 Index futures	NQ	US
Dow Jones Indexes futures	YM	US
CSI 300 Index futures	IF	China
CSI 500 Index futures	IC	China
SSE 50 Index futures	IH	China
Hang Seng Index futures	HSIF	Hong Kong
Nikkei 225 Stock Index futures	NK	Japan
MSCI Singapore Index futures	SGP	Singapore
Nifty 50 Stock Index futures	IN	India

Table A2
Abbreviation of models.

Name of models	Symbol
Discrete Wavelet Transform	DWT
Maximal overlap discrete wavelet transform	MODWT
Complete EEMD with Adaptive Noise	CEEMDAN
Autoregressive Integrated Moving Average model	ARIMA
Long Short Term Memory	LSTM
A hybrid model combining DWT method and ARIMA model	DWT-ARIMA
A hybrid model combining DWT method and LSTM model	DWT-LSTM
A hybrid model combining DWT method, ARIMA model and LSTM model	DWT-ARIMA-LSTM
A hybrid model combining MODWT method and ARIMA model	MODWT-ARIMA
A hybrid model combining MODWT method and LSTM model	MODWT-LSTM
A hybrid model combining MODWT method, ARIMA model and LSTM model	MODWT-ARIMA-LSTM
A hybrid model combining CEEMDAN method and LSTM model	CEEMDAN-LSTM

Table A3
FDAX.

		In sample			Out sample		
		MAE	MAPE	RMSE	MAE	MAPE	RMSE
Window 1	DWT-ARIMA-LSTM	221.838	1.448 %	317.810	227.199	1.539 %	325.879
	DWT-ARIMA	243.269	1.640 %	349.957	253.211	1.712 %	363.661
	MODWT-ARIMA	214.719	1.284 %	303.679	235.863	1.591 %	332.170
	DWT-LSTM	420.716	2.857 %	493.369	644.047	4.188 %	717.594
	MODWT-LSTM	589.723	3.985 %	651.331	912.840	5.936 %	963.155
	CEEMDAN-LSTM	1027.755	6.928 %	1259.086	1549.411	10.050 %	1947.663
	LSTM	1058.036	7.119 %	1151.120	1598.454	10.491 %	1610.029
	ARIMA	234.504	1.680 %	304.273	278.390	1.850 %	347.122
	ARIMA-LSTM	265.958	1.889 %	334.106	329.210	2.173 %	392.921
	MODWT-ARIMA-LSTM	227.756	1.639 %	294.260	249.863	1.660 %	314.650
Window 2	DWT-ARIMA-LSTM	222.601	1.652 %	284.699	223.364	1.674 %	295.770
	DWT-ARIMA	243.372	1.803 %	307.561	243.475	1.822 %	321.782
	MODWT-ARIMA	195.660	1.479 %	244.249	216.109	1.619 %	283.427
	DWT-LSTM	393.671	2.904 %	417.589	402.686	2.951 %	459.037
	MODWT-LSTM	605.431	4.284 %	626.226	621.139	4.584 %	658.192
	CEEMDAN-LSTM	816.716	6.401 %	657.408	887.062	6.577 %	916.630
	LSTM	1318.675	9.390 %	1425.618	1579.315	11.661 %	1612.013
	ARIMA	255.866	1.864 %	321.693	277.228	2.048 %	336.112
	ARIMA-LSTM	287.507	2.085 %	355.410	309.056	2.282 %	371.577
	MODWT-ARIMA-LSTM	233.121	1.705 %	288.548	238.485	1.771 %	290.687

3.4. Forecasting results and discussions

3.4.1. Forecasting results of ARIMA-LSTM

The forecasting results of ARIMA-LSTM, DWT-ARIMA-LSTM, MODWT-ARIMA-LSTM, CEEMDAN-LSTM models for futures closing price series are compared to demonstrate the advantages of our proposed hybrid model. The forecasting results of the hybrid model are shown in Fig. 11. Intuitively, the hybrid model fits the closing price series better than the CEEMDAN-LSTM model and the ARIMA model which is shown in Fig. 9.

Table A4
NQ.

		In sample			Out sample		
		MAE	MAPE	RMSE	MAE	MAPE	RMSE
Window 1	DWT-ARIMA-LSTM	105.599	1.490 %	146.814	111.911	1.552 %	151.256
	DWT-ARIMA	108.851	1.532 %	152.635	115.421	1.594 %	160.025
	MODWT-ARIMA	115.091	1.618 %	158.376	126.602	1.747 %	169.551
	DWT-LSTM	178.523	2.417 %	199.923	264.197	3.511 %	283.536
	MODWT-LSTM	255.257	3.460 %	278.801	333.026	4.405 %	357.985
	CEEMDAN-LSTM	325.966	4.134 %	360.967	326.578	4.298 %	370.795
	LSTM	508.933	6.934 %	564.609	647.532	8.684 %	670.191
	ARIMA	95.273	1.270 %	129.388	107.391	1.476 %	138.129
	ARIMA-LSTM	110.592	1.470 %	146.968	119.079	1.630 %	150.734
	MODWT-ARIMA-LSTM	102.626	1.370 %	137.315	112.429	1.546 %	143.760
Window 2	DWT-ARIMA-LSTM	175.823	2.014 %	250.016	246.046	2.538 %	353.150
	DWT-ARIMA	180.884	2.078 %	264.317	252.917	2.624 %	375.820
	MODWT-ARIMA	181.064	2.084 %	258.090	247.037	2.549 %	357.410
	DWT-LSTM	242.522	2.832 %	297.283	306.522	3.246 %	377.863
	MODWT-LSTM	425.204	4.724 %	472.585	595.151	5.989 %	655.341
	CEEMDAN-LSTM	497.274	5.453 %	557.660	668.583	6.443 %	754.220
	LSTM	1098.374	11.311 %	1300.315	1687.816	15.689 %	2026.234
	ARIMA	197.942	2.271 %	256.874	276.376	2.859 %	366.617
	ARIMA-LSTM	202.564	2.333 %	259.030	277.561	2.877 %	363.514
	MODWT-ARIMA-LSTM	201.517	2.302 %	259.819	280.801	2.883 %	369.295
Window 3	DWT-ARIMA-LSTM	166.746	0.994 %	239.765	181.077	1.276 %	242.984
	DWT-ARIMA	179.176	1.178 %	262.203	201.479	1.417 %	274.110
	MODWT-ARIMA	176.747	1.089 %	251.815	194.421	1.369 %	259.939
	DWT-LSTM	631.561	4.906 %	687.864	1041.933	7.118 %	1094.836
	MODWT-LSTM	943.869	7.343 %	1020.291	1519.183	10.384 %	1594.312
	CEEMDAN-LSTM	1001.312	7.921 %	1073.293	1562.453	10.720 %	1620.711
	LSTM	2905.284	22.113 %	3130.224	4908.675	34.374 %	5000.092
	ARIMA	252.746	2.187 %	310.352	333.694	2.299 %	377.323
	ARIMA-LSTM	210.015	1.450 %	268.405	242.465	1.684 %	291.922
	MODWT-ARIMA-LSTM	206.511	1.428 %	266.148	237.934	1.655 %	286.270
Window 4	DWT-ARIMA-LSTM	232.817	2.057 %	317.976	306.054	2.416 %	397.779
	DWT-ARIMA	242.883	2.144 %	336.108	317.742	2.511 %	415.760
	MODWT-ARIMA	244.346	2.162 %	326.672	320.783	2.536 %	405.490
	DWT-LSTM	534.242	4.383 %	674.788	642.108	4.966 %	750.541
	MODWT-LSTM	756.339	6.218 %	924.693	856.465	6.614 %	963.483
	CEEMDAN-LSTM	1027.411	8.433 %	1169.483	1334.079	10.344 %	1409.405
	LSTM	2077.236	16.677 %	2202.694	2250.883	17.372 %	2377.773
	ARIMA	255.595	2.237 %	329.841	298.918	2.343 %	376.806
	ARIMA-LSTM	252.587	2.257 %	317.333	311.384	2.478 %	377.213
	MODWT-ARIMA-LSTM	232.213	2.079 %	293.263	273.626	2.164 %	329.847

3.4.2. Performance evaluation of hybrid models

The MAE, MAPE and RMSE were used to evaluate the forecasting results of models. The comparison results are shown in Table 9. The WT-ARIMA-LSTM model has lower values of the evaluation indicators for the forecasting results of different futures, indicating that the model has better forecasting performance.

Table 9 also shows the evaluation of the model's in-sample and out-of-sample forecasting results for each stock index futures. From the statistical results in the table, the in-sample forecasting accuracy is slightly higher than the out-of-sample forecasting accuracy, indicating that the forecasting model has been effectively trained and can be better applied to out-of-sample data. In addition, considering the different sample intervals selected for different stock index futures, the in-sample and out-of-sample forecast evaluation statistics for each time window are presented in the Appendix, which can be found in Appendix Table A3-A10 (IN and SGP only contain one time window, so they are not shown in the appendix).

By comparing the prediction results of the original model (ARIMA/LSTM/ARIMA-LSTM), DWT hybrid model, MODWT hybrid model and CEEMDAN hybrid model, it can be seen that the introduction of data decomposition methods can effectively improve the prediction ability of the models under the MAE, MAPE and RMSE metrics. In addition, the prediction models based on the DWT method slightly outperformed those based on the MODWT method in most of the samples, indicating that the DWT method can better capture the data characteristics of different frequencies. Combined with Figs. 4 and 6 and related contents in Table 2 and 3, this paper concludes that although MODWT has more robust edge effects, the DWT method has a better denoising function and the approximate signal derived by the DWT method can better characterize the long-term trend of the data.

In summary, firstly, the introduction of the data decomposition technique can effectively improve the performance of the prediction model. Secondly, among the DWT, MODWT and CEEMDAN methods, the DWT method has the best performance improvement of the prediction model, and the MODWT method is slightly worse than the DWT method. Finally, the prediction performance of the hybrid model is better than the single model, while the ARIMA model performs better than the LSTM model in the dataset of this work.

Table A5
YM.

		In sample			Out sample		
		MAE	MAPE	RMSE	MAE	MAPE	RMSE
Window 1	DWT-ARIMA-LSTM	311.096	1.240 %	450.245	391.540	1.544 %	520.913
	DWT-ARIMA	340.135	1.356 %	489.180	432.378	1.706 %	566.508
	MODWT-ARIMA	342.268	1.363 %	485.270	440.104	1.735 %	567.115
	DWT-LSTM	2588.825	9.701 %	2636.225	2833.300	10.966 %	2884.704
	MODWT-LSTM	1234.169	4.593 %	1297.994	1493.105	5.767 %	1550.472
	CEEMDAN-LSTM	441.280	2.083 %	604.183	581.671	2.278 %	699.152
	LSTM	2641.710	9.940 %	2712.549	2868.232	11.128 %	2927.728
	ARIMA	982.441	3.721 %	1052.195	982.656	3.807 %	1075.213
	ARIMA-LSTM	1047.273	4.142 %	1125.501	1198.811	4.653 %	1288.543
	MODWT-ARIMA-LSTM	581.931	2.313 %	672.131	619.184	2.409 %	722.802
Window 2	DWT-ARIMA-LSTM	432.190	1.742 %	719.643	553.284	2.245 %	983.528
	DWT-ARIMA	454.668	1.826 %	734.053	569.202	2.296 %	972.852
	MODWT-ARIMA	504.865	2.014 %	754.664	667.461	2.664 %	1017.204
	DWT-LSTM	360.409	1.403 %	825.733	1266.198	5.012 %	1598.162
	MODWT-LSTM	897.435	3.417 %	1129.101	1182.304	4.592 %	1359.582
	CEEMDAN-LSTM	1689.730	6.519 %	1908.332	1974.836	7.399 %	2112.900
	LSTM	2726.535	10.087 %	3201.077	2849.275	10.830 %	3251.890
	ARIMA	695.032	2.711 %	1067.668	790.978	3.105 %	1082.889
	ARIMA-LSTM	601.725	2.356 %	1027.261	750.241	2.951 %	1063.924
	MODWT-ARIMA-LSTM	656.497	2.596 %	863.889	731.063	2.880 %	1053.739
Window 3	DWT-ARIMA-LSTM	254.353	0.610 %	271.061	300.177	0.931 %	407.011
	DWT-ARIMA	257.727	0.616 %	292.076	310.648	0.967 %	425.417
	MODWT-ARIMA	211.744	0.463 %	248.037	291.384	0.908 %	402.554
	DWT-LSTM	3335.471	11.155 %	3584.387	4197.025	12.484 %	4441.669
	MODWT-LSTM	2219.737	7.386 %	2332.316	2877.345	8.614 %	2983.639
	CEEMDAN-LSTM	2476.361	8.103 %	2724.608	3358.028	9.980 %	3598.994
	LSTM	3168.646	8.642 %	3810.559	3324.365	9.702 %	4436.617
	ARIMA	676.499	1.627 %	720.443	757.302	2.295 %	834.525
	ARIMA-LSTM	595.018	1.379 %	636.811	712.766	2.168 %	795.655
	MODWT-ARIMA-LSTM	728.101	2.493 %	858.174	824.561	2.496 %	895.977
Window 4	DWT-ARIMA-LSTM	443.845	1.495 %	658.734	518.777	1.577 %	695.292
	DWT-ARIMA	459.244	1.548 %	683.533	528.457	1.601 %	731.068
	MODWT-ARIMA	459.357	1.523 %	666.963	507.868	1.540 %	685.635
	DWT-LSTM	3548.086	11.526 %	3750.451	4191.478	12.563 %	4259.001
	MODWT-LSTM	3016.036	9.603 %	3147.866	4141.139	12.434 %	4211.307
	CEEMDAN-LSTM	3936.964	12.363 %	4153.006	5838.401	17.562 %	5896.513
	LSTM	5052.772	16.145 %	5451.070	7014.758	20.998 %	7362.836
	ARIMA	1290.922	4.202 %	1405.794	1703.338	5.106 %	1801.097
	ARIMA-LSTM	1161.301	3.823 %	1299.306	1433.214	4.294 %	1555.579
	MODWT-ARIMA-LSTM	861.652	2.813 %	1014.125	1043.432	3.125 %	1188.339
Window 5	DWT-ARIMA-LSTM	458.819	1.346 %	534.036	476.693	1.422 %	585.018
	DWT-ARIMA	525.678	1.701 %	717.058	591.185	1.760 %	730.054
	MODWT-ARIMA	396.057	1.034 %	419.276	422.939	1.260 %	514.539
	DWT-LSTM	1325.403	3.413 %	1249.745	1924.269	5.694 %	1996.768
	MODWT-LSTM	1439.952	3.921 %	1366.133	1767.792	5.231 %	1837.063
	CEEMDAN-LSTM	2150.309	6.081 %	1855.023	2412.951	7.155 %	2446.305
	LSTM	3878.891	10.877 %	3502.533	3923.980	11.640 %	3942.654
	ARIMA	208.861	0.398 %	245.350	492.097	1.458 %	580.870
	ARIMA-LSTM	331.885	0.740 %	407.833	562.509	1.666 %	674.835
	MODWT-ARIMA-LSTM	303.764	0.730 %	346.002	470.696	1.396 %	557.595

4. Timing trading strategy construction and evaluation

4.1. Timing trading strategy construction

To further evaluate the forecasting performance of the model, we constructed a timing strategy based on the forecasting results and back-testing the trading results. The basic idea of the strategy is to trigger a buy and sell trade signal based on the difference between the forecast price and the previous day's closing price, and to take a long and short position at the daily opening time and close it at the close of the day. This is done as follows: a long or short position is opened at the opening time of day t and closed at the close of the day, based on the forecast of the closing price on day t, y_t^*, made on day $t-1$ and the actual closing price on day $t-1$, y_{t-1}, as follows:

Table A6
IF.

		In sample			Out sample		
		MAE	MAPE	RMSE	MAE	MAPE	RMSE
Window 1	DWT-ARIMA-LSTM	38.752	1.321 %	53.222	55.464	1.731 %	77.010
	DWT-ARIMA	38.052	1.306 %	53.925	56.879	1.774 %	78.708
	MODWT-ARIMA	56.006	1.871 %	86.456	73.625	2.291 %	108.015
	DWT-LSTM	67.659	2.247 %	71.982	85.314	2.610 %	95.732
	MODWT-LSTM	121.601	3.983 %	127.545	147.237	4.489 %	159.648
	CEEMDAN-LSTM	205.849	6.596 %	209.955	219.973	6.778 %	228.053
	LSTM	382.991	12.496 %	379.948	436.689	13.472 %	441.848
	ARIMA	66.498	2.165 %	79.799	82.261	2.523 %	99.391
	ARIMA-LSTM	63.744	2.082 %	76.273	78.015	2.402 %	94.493
	MODWT-ARIMA-LSTM	44.434	1.532 %	67.623	63.296	1.976 %	89.345
Window 2	DWT-ARIMA-LSTM	24.005	0.651 %	27.091	35.662	0.981 %	46.742
	DWT-ARIMA	24.480	0.664 %	28.567	37.177	1.023 %	48.794
	MODWT-ARIMA	34.714	0.942 %	45.151	47.824	1.315 %	65.044
	DWT-LSTM	39.718	1.136 %	47.639	53.798	1.502 %	66.769
	MODWT-LSTM	114.504	3.188 %	110.805	130.167	3.591 %	134.044
	CEEMDAN-LSTM	35.453	0.967 %	42.105	67.866	1.875 %	77.165
	LSTM	514.907	14.535 %	552.675	526.746	14.801 %	567.213
	ARIMA	37.260	0.994 %	45.530	50.444	1.365 %	63.131
	ARIMA-LSTM	27.695	0.742 %	33.480	41.000	1.117 %	51.391
	MODWT-ARIMA-LSTM	54.047	1.474 %	64.258	63.452	1.736 %	79.035
Window 3	DWT-ARIMA-LSTM	74.560	2.099 %	98.269	75.664	2.128 %	103.818
	DWT-ARIMA	79.334	2.225 %	109.606	80.567	2.259 %	114.200
	MODWT-ARIMA	118.763	3.356 %	166.116	122.463	3.465 %	168.304
	DWT-LSTM	41.605	1.182 %	50.631	51.393	1.437 %	65.279
	MODWT-LSTM	66.129	1.865 %	72.441	84.228	2.342 %	95.853
	CEEMDAN-LSTM	111.505	3.106 %	118.061	123.792	3.449 %	135.331
	LSTM	247.250	7.090 %	247.138	293.943	8.344 %	301.364
	ARIMA	68.063	1.928 %	87.767	73.079	2.060 %	95.588
	ARIMA-LSTM	71.404	2.017 %	94.901	74.663	2.102 %	100.351
	MODWT-ARIMA-LSTM	104.981	2.960 %	135.026	105.762	2.995 %	136.354
Window 4	DWT-ARIMA-LSTM	58.841	1.551 %	76.774	61.954	1.652 %	84.320
	DWT-ARIMA	60.985	1.605 %	81.017	64.575	1.719 %	88.786
	MODWT-ARIMA	75.843	1.982 %	100.842	80.125	2.123 %	109.088
	DWT-LSTM	138.715	3.670 %	154.910	147.370	3.887 %	158.572
	MODWT-LSTM	213.096	5.641 %	225.697	222.581	5.871 %	228.797
	CEEMDAN-LSTM	286.371	7.605 %	299.427	307.828	8.127 %	315.769
	LSTM	463.824	12.209 %	465.489	469.573	12.463 %	479.459
	ARIMA	45.458	1.201 %	60.382	52.629	1.409 %	70.663
	ARIMA-LSTM	55.165	1.444 %	70.570	60.045	1.593 %	78.442
	MODWT-ARIMA-LSTM	69.178	1.809 %	82.297	73.902	1.956 %	90.880
Window 5	DWT-ARIMA-LSTM	88.913	2.093 %	139.029	95.259	2.187 %	150.709
	DWT-ARIMA	93.996	2.210 %	148.368	100.835	2.313 %	160.866
	MODWT-ARIMA	119.116	2.822 %	195.040	126.737	2.926 %	210.357
	DWT-LSTM	149.274	3.318 %	175.107	162.235	3.509 %	189.385
	MODWT-LSTM	291.653	6.526 %	311.328	320.773	7.017 %	341.192
	CEEMDAN-LSTM	376.970	8.524 %	394.991	416.391	9.217 %	432.038
	LSTM	509.326	11.387 %	536.530	524.844	11.514 %	552.313
	ARIMA	81.880	1.929 %	123.717	85.336	1.946 %	131.729
	ARIMA-LSTM	86.088	2.033 %	130.337	90.619	2.079 %	139.733
	MODWT-ARIMA-LSTM	114.131	2.682 %	161.732	121.637	2.785 %	173.810
Window 6	DWT-ARIMA-LSTM	74.721	1.479 %	105.801	76.238	1.516 %	106.276
	DWT-ARIMA	78.112	1.541 %	108.795	79.576	1.582 %	109.094
	MODWT-ARIMA	101.439	1.979 %	141.284	102.870	2.048 %	142.375
	DWT-LSTM	259.885	5.262 %	272.416	291.122	5.798 %	300.493
	MODWT-LSTM	311.532	6.366 %	323.079	335.951	6.698 %	343.433
	CEEMDAN-LSTM	359.459	7.359 %	373.867	385.556	7.697 %	392.906
	LSTM	667.226	13.731 %	694.138	709.916	14.121 %	735.627
	ARIMA	77.949	1.580 %	98.723	80.464	1.597 %	99.635
	ARIMA-LSTM	59.828	1.123 %	77.977	60.793	1.209 %	80.833
	MODWT-ARIMA-LSTM	88.526	1.682 %	112.241	88.907	1.780 %	114.179
Window 7	DWT-ARIMA-LSTM	73.816	1.830 %	98.038	74.311	1.836 %	100.304
	DWT-ARIMA	79.571	1.969 %	105.370	79.831	1.969 %	107.624
	MODWT-ARIMA	91.817	2.254 %	133.661	94.136	2.309 %	137.684
	DWT-LSTM	106.201	2.663 %	113.338	114.320	2.805 %	125.320
	MODWT-LSTM	143.243	3.593 %	148.065	157.192	3.863 %	165.767
	CEEMDAN-LSTM	166.589	4.147 %	172.592	186.847	4.572 %	196.331
	LSTM	322.501	8.081 %	319.550	347.797	8.585 %	351.060

(continued on next page)

Table A6 (*continued*)

		In sample			Out sample		
		MAE	MAPE	RMSE	MAE	MAPE	RMSE
	ARIMA	65.278	1.609 %	82.355	66.364	1.630 %	85.125
	ARIMA-LSTM	61.863	1.526 %	76.580	63.244	1.558 %	80.327
	MODWT-ARIMA-LSTM	81.484	2.020 %	102.677	83.779	2.072 %	106.921

Table A7
IH.

		In sample			Out sample		
		MAE	MAPE	RMSE	MAE	MAPE	RMSE
Window 1	DWT-ARIMA-LSTM	56.203	1.610 %	74.448	56.497	1.632 %	75.850
	DWT-ARIMA	58.294	1.672 %	76.058	58.512	1.697 %	77.483
	MODWT-ARIMA	60.679	1.746 %	77.324	61.152	1.765 %	78.535
	DWT-LSTM	122.236	3.529 %	136.694	127.476	3.634 %	140.698
	MODWT-LSTM	174.914	5.072 %	190.425	182.655	5.230 %	197.521
	CEEMDAN-LSTM	264.094	7.767 %	271.678	272.250	7.894 %	278.823
	LSTM	194.711	5.708 %	200.922	208.867	6.057 %	213.483
	ARIMA	167.513	4.861 %	183.648	178.024	5.106 %	193.675
	ARIMA-LSTM	113.277	3.288 %	132.190	117.340	3.356 %	135.546
	MODWT-ARIMA-LSTM	95.821	2.683 %	112.424	97.102	2.778 %	114.485
Window 2	DWT-ARIMA-LSTM	48.063	1.736 %	60.656	48.989	1.740 %	63.187
	DWT-ARIMA	47.480	1.720 %	60.204	48.763	1.727 %	63.006
	MODWT-ARIMA	52.758	1.890 %	65.328	53.600	1.900 %	67.523
	DWT-LSTM	43.372	1.558 %	53.759	51.593	1.771 %	62.971
	MODWT-LSTM	71.301	2.547 %	80.531	81.834	2.813 %	92.272
	CEEMDAN-LSTM	133.619	4.708 %	148.609	147.380	5.051 %	161.914
	LSTM	171.619	5.999 %	182.319	173.668	6.193 %	183.518
	ARIMA	22.294	0.905 %	32.320	37.161	1.323 %	48.582
	ARIMA-LSTM	27.546	1.065 %	37.400	36.993	1.322 %	48.269
	MODWT-ARIMA-LSTM	31.654	1.183 %	42.202	40.395	1.423 %	52.166
Window 3	DWT-ARIMA-LSTM	38.115	1.498 %	45.625	40.015	1.525 %	49.354
	DWT-ARIMA	52.538	1.980 %	72.686	52.815	2.016 %	73.180
	MODWT-ARIMA	43.160	1.690 %	46.261	44.956	1.711 %	50.240
	DWT-LSTM	34.755	1.413 %	37.503	41.655	1.582 %	46.594
	MODWT-LSTM	53.074	2.147 %	54.046	62.813	2.386 %	66.300
	CEEMDAN-LSTM	45.409	1.927 %	45.864	66.183	2.517 %	68.664
	LSTM	254.491	9.538 %	257.010	269.556	10.246 %	270.183
	ARIMA	14.170	0.650 %	17.212	25.717	0.978 %	32.004
	ARIMA-LSTM	18.768	0.796 %	19.818	26.556	1.012 %	30.502
	MODWT-ARIMA-LSTM	17.840	0.754 %	21.570	25.758	0.978 %	31.874

$$\begin{cases} y_t^* > y_{t-1} + MAE, Openalongposition \\ y_t^* < y_{t-1} - MAE, Openashortposition \\ y_{t-1} - MAE \leq y_t^* \leq y_{t-1} + MAE, Cashholdings \end{cases} \tag{31}$$

where, MAE represents the average absolute error of the previous 20 days of forecasts, introduced to filter out subtle errors.

4.2. Strategy evaluation

Ignoring factors such as transaction fees and leverage, and setting the initial capital to 1, the net value curves of the timing strategy and the benchmark strategy, which is set as a buy-and-hold strategy, are calculated respectively for the back-testing period, as shown in Fig. 12. The timing strategies outperformed the buy-and-hold strategy for all returns except IN. It can also be seen that the timing strategy has a much flatter trend.

The strategy backtesting results are shown in Table 10. All of the underlying timing strategies had higher annualised returns than the buy-and-hold strategy, except for the IN timing strategy, which had a slightly lower annualised return of 9.056 % than the buy-and-hold strategy, which had an annualised return of 11.190 %. The strategy has significant advantages in terms of volatility and retracement.

Table A8
IC.

		In sample			Out sample		
		MAE	MAPE	RMSE	MAE	MAPE	RMSE
Window 1	DWT-ARIMA-LSTM	86.768	1.291 %	114.397	87.625	1.310 %	115.726
	DWT-ARIMA	95.330	1.415 %	123.781	96.100	1.433 %	125.114
	MODWT-ARIMA	91.570	1.363 %	125.128	92.509	1.384 %	126.430
	DWT-LSTM	322.611	4.733 %	340.023	332.575	4.921 %	350.567
	MODWT-LSTM	472.874	6.950 %	490.284	484.482	7.172 %	502.825
	CEEMDAN-LSTM	372.536	5.550 %	379.543	376.903	5.640 %	384.853
	LSTM	179.682	2.605 %	242.351	180.436	2.606 %	243.864
	ARIMA	314.627	4.679 %	340.184	316.126	4.690 %	341.400
	ARIMA-LSTM	291.556	4.295 %	317.358	295.103	4.370 %	321.038
	MODWT-ARIMA-LSTM	187.993	2.791 %	212.708	189.495	2.827 %	214.496
Window 2	DWT-ARIMA-LSTM	101.339	1.633 %	136.649	101.484	1.636 %	136.952
	DWT-ARIMA	103.306	1.664 %	139.533	103.538	1.669 %	139.965
	MODWT-ARIMA	109.372	1.768 %	147.453	109.495	1.771 %	147.734
	DWT-LSTM	85.489	1.351 %	109.337	95.313	1.514 %	120.379
	MODWT-LSTM	123.235	1.920 %	141.545	136.147	2.134 %	156.042
	CEEMDAN-LSTM	240.763	3.799 %	259.064	245.626	3.880 %	264.506
	LSTM	393.000	6.168 %	407.392	397.813	6.243 %	411.502
	ARIMA	164.929	2.603 %	195.711	167.218	2.639 %	198.058
	ARIMA-LSTM	140.350	2.217 %	171.211	145.183	2.297 %	176.206
	MODWT-ARIMA-LSTM	107.443	1.715 %	136.084	109.820	1.755 %	138.603
Window 3	DWT-ARIMA-LSTM	161.968	2.766 %	183.435	163.129	2.787 %	184.194
	DWT-ARIMA	179.240	3.060 %	198.773	180.659	3.086 %	199.698
	MODWT-ARIMA	164.874	2.810 %	169.555	165.944	2.830 %	169.815
	DWT-LSTM	49.007	0.837 %	68.913	56.351	0.957 %	78.425
	MODWT-LSTM	35.472	0.608 %	52.904	45.922	0.779 %	66.109
	CEEMDAN-LSTM	81.330	1.389 %	95.248	87.793	1.491 %	102.539
	LSTM	328.829	5.596 %	333.128	330.667	5.634 %	333.963
	ARIMA	100.866	1.730 %	118.185	103.689	1.772 %	121.421
	ARIMA-LSTM	102.869	1.760 %	114.736	106.873	1.823 %	119.610
	MODWT-ARIMA-LSTM	85.053	1.461 %	117.819	87.101	1.492 %	120.030

5. Robustness test

5.1. Strategy robustness tests under different market conditions

To verify the robustness of the timing strategy, we analyzed the performance of the timing trading strategy under the three different market quotation periods respectively. The upside periods are indicated by a light gray box. The downside periods are indicated by a dark gray box and the oscillation periods are represented in white. The specific market intervals are shown in Fig. 13.

The overall performance of this strategy during the upside, downside and oscillation periods is shown in Table 11. It is able to achieve a solid return performance even during the downside and oscillation periods of the market because the timing strategy operates in both long and short directions. Although the performance of this strategy was average during the upside, it was able to be applied well to different market quotation periods and achieve more robust returns.

Specifically, in terms of returns, timing strategies do not consistently outperform buy-and-hold strategies in upside periods. The buy-and-hold strategies on NQ, YM, IC and IN have higher annualized returns than the timing strategies while the buy-and-hold strategies on the other underlying have lower annualized returns than the timing strategies. In downside periods and shocks, timing strategies mostly outperform buy-and-hold strategies. In terms of risk, the volatility and maximum retracement metrics of the timing strategy are consistently better than those of the buy-and-hold strategy in all three different market conditions. Finally, the timing strategy's the Sharpe ratio consistently outperforms the buy-and-hold strategy in all three different market conditions. Overall, the timing strategy has consistently outperformed the buy-and-hold strategy over time.

5.2. Strategy robustness tests under COVID-19 epidemic shocks

Combined with the preliminary analysis of the impact of the COVID-19 epidemic on futures closing price movements in Fig. 3, it is suggested that the epidemic shock may have an impact on the data structure. Given the time span of the sample (COVID-19 outbreak after January 2020), a total of five futures, NQ, YM, IF, HSIF and NK, were selected for this part of the test.

The Kolmogorov-Smirnov test (KS test) was used to compare whether the distribution of the two groups of samples was the same before and after the epidemic. The statistical results of the KS test are shown in Table 12. The p-values are all less than 0.05, so the null hypothesis is rejected and the distribution of the closing price series before and after the COVID-19 epidemic is different.

To test the stability of the model in samples with different data structures, the prediction performance of the prediction model before and after the epidemic was examined, and the results are shown in Table 13. It can be seen that the prediction accuracy in the

Table A9
HSIF.

		In sample			Out sample		
		MAE	MAPE	RMSE	MAE	MAPE	RMSE
Window 1	DWT-ARIMA-LSTM	446.606	1.655 %	583.811	450.315	1.663 %	591.640
	DWT-ARIMA	447.319	1.676 %	604.856	454.543	1.679 %	617.176
	MODWT-ARIMA	473.310	1.732 %	615.295	475.015	1.748 %	620.814
	DWT-LSTM	1080.506	3.921 %	1166.669	1111.385	4.071 %	1193.817
	MODWT-LSTM	1294.444	4.669 %	1357.540	1325.405	4.824 %	1383.355
	CEEMDAN-LSTM	1727.352	6.252 %	1789.804	1805.517	6.585 %	1860.330
	LSTM	1787.044	6.685 %	1822.583	2028.041	7.416 %	2071.818
	ARIMA	589.732	2.139 %	712.494	620.841	2.269 %	739.776
	ARIMA-LSTM	738.500	2.681 %	850.902	787.063	2.877 %	891.473
	MODWT-ARIMA-LSTM	504.773	1.830 %	619.675	505.347	1.849 %	627.653
Window 2	DWT-ARIMA-LSTM	480.001	1.872 %	659.472	482.785	1.912 %	666.109
	DWT-ARIMA	500.810	1.958 %	683.606	504.308	2.003 %	687.257
	MODWT-ARIMA	523.630	2.047 %	733.113	530.737	2.106 %	748.562
	DWT-LSTM	307.407	1.308 %	488.229	394.395	1.588 %	565.063
	MODWT-LSTM	294.115	1.274 %	484.951	409.481	1.650 %	586.352
	CEEMDAN-LSTM	218.165	0.965 %	380.031	382.387	1.522 %	536.559
	LSTM	1887.279	7.510 %	1943.526	2010.311	7.818 %	2084.417
	ARIMA	429.680	1.737 %	582.854	439.965	1.747 %	591.413
	ARIMA-LSTM	516.669	2.088 %	653.367	529.222	2.101 %	667.047
	MODWT-ARIMA-LSTM	449.221	1.808 %	598.892	456.488	1.812 %	606.052
Window 3	DWT-ARIMA-LSTM	452.234	1.685 %	584.185	454.429	1.690 %	590.601
	DWT-ARIMA	505.367	1.881 %	652.888	508.264	1.896 %	655.068
	MODWT-ARIMA	477.769	1.783 %	617.191	480.244	1.789 %	624.840
	DWT-LSTM	320.334	1.182 %	416.651	380.334	1.396 %	484.293
	MODWT-LSTM	274.065	1.020 %	368.166	358.289	1.318 %	461.037
	CEEMDAN-LSTM	174.578	0.653 %	248.086	296.350	1.086 %	388.108
	LSTM	1916.838	7.072 %	1972.221	2000.291	7.345 %	2073.324
	ARIMA	394.647	1.465 %	499.298	406.312	1.506 %	515.884
	ARIMA-LSTM	454.983	1.704 %	579.234	471.586	1.761 %	598.365
	MODWT-ARIMA-LSTM	384.315	1.433 %	506.249	397.575	1.478 %	522.955
Window 4	DWT-ARIMA-LSTM	468.330	2.102 %	622.452	468.726	2.166 %	622.719
	DWT-ARIMA	491.644	2.191 %	664.245	491.820	2.253 %	664.532
	MODWT-ARIMA	509.926	2.288 %	665.635	512.708	2.366 %	665.673
	DWT-LSTM	340.905	1.694 %	433.491	385.209	1.797 %	487.316
	MODWT-LSTM	322.161	1.622 %	406.068	381.949	1.779 %	478.996
	CEEMDAN-LSTM	410.131	1.991 %	485.929	475.821	2.162 %	575.280
	LSTM	1574.437	7.242 %	1736.247	1682.435	7.434 %	1846.976
	ARIMA	498.489	2.276 %	615.176	503.646	2.369 %	616.863
	ARIMA-LSTM	439.439	2.110 %	548.498	454.353	2.118 %	567.586
	MODWT-ARIMA-LSTM	505.059	2.292 %	617.467	511.369	2.388 %	618.252
Window 5	DWT-ARIMA-LSTM	560.172	3.088 %	700.450	576.190	3.293 %	714.103
	DWT-ARIMA	589.675	3.240 %	733.954	606.332	3.453 %	746.863
	MODWT-ARIMA	587.808	3.215 %	737.596	602.496	3.417 %	749.370
	DWT-LSTM	482.507	2.823 %	612.044	493.172	2.924 %	628.588
	MODWT-LSTM	635.218	3.404 %	747.101	637.958	3.572 %	756.401
	CEEMDAN-LSTM	636.946	3.665 %	760.945	649.831	3.802 %	794.375
	LSTM	616.021	3.754 %	728.198	780.302	4.222 %	889.871
	ARIMA	401.075	2.297 %	533.377	412.527	2.351 %	544.358
	ARIMA-LSTM	403.466	2.388 %	531.339	423.102	2.417 %	551.521
	MODWT-ARIMA-LSTM	474.335	2.606 %	578.651	475.442	2.727 %	580.718

two pre-epidemic and post-epidemic samples is almost the same under the three indicators of MAE, MAPE and RMSE, which indicates that the prediction model in this paper can be better adapted to the samples with different data results.

The performance of the timing strategy before and after the epidemic was further examined and the results are shown in Table 14. In terms of returns, NQ, YM and IF have significantly higher returns in the pre-epidemic period than in the post-epidemic period, while the other two underlying strategies have higher returns in the post-epidemic period. In terms of risk, the volatility of the strategies is significantly higher at the beginning of the outbreak, which is the main reason for the inconsistent returns of the pre- and post-epidemic strategies.

Overall, most of the underlying timing strategies outperformed the buy-and-hold strategy before and after COVID-19. Specifically, in terms of returns, the timing strategy outperformed the buy-and-hold strategy in most periods. In terms of risk, both the volatility and maximum retracement metrics of the timing strategy significantly outperformed the buy-and-hold strategy. Thus, the strategy was able to maintain a relatively robust performance in the face of the COVID-19 outbreak shock.

Table A10
NX.

		In sample			Out sample		
		MAE	MAPE	RMSE	MAE	MAPE	RMSE
Window 1	DWT-ARIMA-LSTM	334.873	1.563 %	459.213	339.691	1.593 %	464.572
	DWT-ARIMA	372.288	1.739 %	506.716	382.511	1.795 %	516.713
	MODWT-ARIMA	380.978	1.780 %	503.561	386.080	1.813 %	508.267
	DWT-LSTM	1283.442	6.048 %	1341.569	1380.428	6.443 %	1435.907
	MODWT-LSTM	2267.258	10.684 %	2334.089	2399.996	11.210 %	2477.146
	CEEMDAN-LSTM	2489.865	11.611 %	2551.480	2564.372	12.021 %	2625.528
	LSTM	4202.637	19.598 %	4535.253	4669.977	21.830 %	4942.561
	ARIMA	1637.640	7.710 %	1721.785	1651.052	7.722 %	1747.113
	ARIMA-LSTM	2459.943	11.428 %	2564.109	2468.406	11.537 %	2577.518
	MODWT-ARIMA-LSTM	1237.744	5.837 %	1350.923	1253.759	5.871 %	1361.686
Window 2	DWT-ARIMA-LSTM	395.130	1.870 %	621.623	407.180	1.934 %	650.858
	DWT-ARIMA	398.904	1.885 %	598.950	407.600	1.933 %	618.276
	MODWT-ARIMA	461.738	2.166 %	682.278	477.324	2.244 %	713.979
	DWT-LSTM	993.212	4.454 %	1070.680	1084.046	4.875 %	1161.431
	MODWT-LSTM	664.580	3.065 %	763.157	939.580	4.313 %	1045.218
	CEEMDAN-LSTM	574.044	2.626 %	667.461	790.238	3.621 %	881.592
	LSTM	2116.612	9.368 %	2095.396	2231.322	9.949 %	2307.836
	ARIMA	217.233	1.072 %	458.365	402.328	1.909 %	630.807
	ARIMA-LSTM	322.271	1.489 %	488.222	586.835	2.698 %	743.572
	MODWT-ARIMA-LSTM	321.509	1.544 %	559.062	445.046	2.100 %	664.162
Window 3	DWT-ARIMA-LSTM	392.105	1.390 %	532.471	398.965	1.421 %	533.984
	DWT-ARIMA	405.080	1.430 %	534.397	411.423	1.465 %	534.809
	MODWT-ARIMA	405.380	1.377 %	532.973	405.512	1.440 %	538.304
	DWT-LSTM	2284.653	8.260 %	2344.415	2414.105	8.497 %	2466.320
	MODWT-LSTM	2546.027	8.995 %	2623.841	2599.879	9.138 %	2638.097
	CEEMDAN-LSTM	2895.095	10.449 %	2963.658	3077.754	10.813 %	3122.732
	LSTM	4785.365	17.199 %	5112.396	5121.820	17.955 %	5402.315
	ARIMA	591.630	1.908 %	682.766	675.939	2.396 %	790.446
	ARIMA-LSTM	719.906	2.277 %	797.218	857.601	3.034 %	961.402
	MODWT-ARIMA-LSTM	789.389	2.640 %	877.070	818.410	2.897 %	918.135
Window 4	DWT-ARIMA-LSTM	408.306	1.519 %	547.376	415.866	1.527 %	550.928
	DWT-ARIMA	437.716	1.641 %	578.570	447.648	1.642 %	586.224
	MODWT-ARIMA	430.195	1.567 %	569.293	434.424	1.592 %	569.754
	DWT-LSTM	2220.305	8.194 %	2274.880	2301.277	8.350 %	2343.473
	MODWT-LSTM	2588.234	9.522 %	2658.246	2633.414	9.568 %	2674.018
	CEEMDAN-LSTM	3627.591	13.373 %	3686.024	3879.057	14.118 %	3910.719
	LSTM	6229.105	22.941 %	6516.088	6708.051	24.433 %	6939.018
	ARIMA	615.733	2.108 %	691.780	678.586	2.465 %	779.619
	ARIMA-LSTM	590.091	1.962 %	670.806	713.893	2.593 %	823.213
	MODWT-ARIMA-LSTM	543.603	1.876 %	654.243	596.999	2.172 %	715.030
Window 5	DWT-ARIMA-LSTM	433.201	1.638 %	548.683	440.331	1.641 %	549.360
	DWT-ARIMA	369.841	1.350 %	492.909	375.148	1.395 %	501.976
	MODWT-ARIMA	302.674	1.096 %	385.203	318.069	1.181 %	410.540
	DWT-LSTM	663.426	2.355 %	728.387	804.868	2.941 %	879.282
	MODWT-LSTM	1023.854	3.647 %	1073.735	1163.774	4.261 %	1228.229
	CEEMDAN-LSTM	1454.795	5.229 %	1488.546	1595.177	5.843 %	1659.964
	LSTM	3404.212	12.326 %	3368.834	3564.035	13.103 %	3594.506
	ARIMA	342.032	1.168 %	459.999	405.775	1.475 %	537.749
	ARIMA-LSTM	306.695	1.015 %	359.496	412.944	1.509 %	499.948
	MODWT-ARIMA-LSTM	273.989	0.944 %	336.616	337.059	1.234 %	413.937

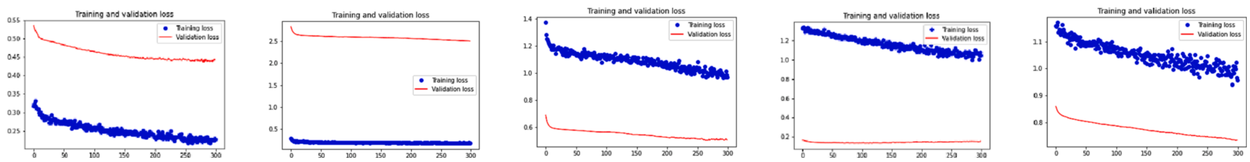

Fig. A1. Plot of training and validation error changes.

6. Conclusions

A new hybrid model combining WT, ARIMA and LSTM models is proposed to predict share price index futures. The wavelet transform can decompose complex share price index futures into a series of different scale sequences that extract deep features from the data. The ARIMA, which excels in handling linear relationships between data, is the vastly applied to time series problems and the LSTM is the first choice for learning the long-term dependence information of data. It can be found that the proposed model performs better and has good adaptability in different datasets. In addition, a timing trading strategy based on the forecasting results was proposed in this work. Compared with the buy-and-hold strategy, the timing trading strategy performed better and had good adaptability.

In this work, the ARIMA, LSTM, DWT-ARIMA, MODWT-ARIMA, DWT-LSTM, MODWT-LSTM, CEEMDAN-LSTM, ARIMA-LSTM, DWT-ARIMA-LSTM and MODWT-ARIMA-LSTM models have been applied to forecast the closing prices of FDAX, NQ, YM, IF, IC, IH, HSIF, NK, SGP and IN. The DWT-ARIMA-LSTM hybrid model has the best forecasting performance for most of the datasets. Specifically, the DWT hybrid model and the MODWT hybrid model have the highest prediction accuracy under the three metrics of MAE, MAPE and RMSE. The DWT-ARIMA-LSTM model performs slightly better than the MODWT-ARIMA-LSTM model on most of the data sets. This indicates that the introduction of the wavelet decomposition technique effectively extracts the data features of different frequencies in the samples. Furthermore, from the comparison of ARIMA and its derivative models with LSTM and its derivative models, the ARIMA model outperforms the LSTM model on the futures closing price series.

The DWT method has better applicability in forecasting models of futures closing price series. the MODWT method is a wavelet decomposition method with more robust boundary effects derived from the DWT method. From the decomposed wavelet waveform, the approximate signal obtained by the DWT method decomposition has lower volatility. At the same time, the approximate signal obtained by the DWT method can better characterize the original signal. The result indicates that the noise reduction function of the MODWT method is inferior to that of the DWT method, thus affecting the prediction performance of the prediction model.

In addition, in this work, a timing trading strategy was constructed based on the prediction results and compared with a buy-and-hold strategy. The results show that the timing trading strategy has significant advantages in terms of volatility and retracement. All of the underlying timing strategies had higher annualized returns than the buy-and-hold strategy, except for the IN's timing strategy, which had a slightly lower annualized return of 9.056 % than the buy-and-hold strategy, which had an annualized return of 11.190 %.

In the robustness test, the performance of the strategy in different quotes is first examined. It is able to achieve a solid return performance even during the downside and oscillation periods of the market because the timing strategy operates in both long and short directions. Although the performance of this strategy was average during the upside, it was able to be applied well to different market quotation periods and achieve more robust returns. Specifically, in terms of returns, timing strategies do not consistently outperform buy-and-hold strategies in upside periods. In downside periods and during shocks, timing strategies mostly outperform buy-and-hold strategies. In terms of risk, the volatility and maximum retracement metrics of the timing strategy are consistently better than those of the buy-and-hold strategy in all three different market conditions.

Finally, the effect of the covid-19 epidemic shock on the experiments in this work was examined. Firstly, the KS test showed that the distribution of samples before and after the epidemic was different. Second, the prediction accuracy before and after the epidemic was examined, and the results showed that the prediction model can effectively adapt to samples with different distributions. Finally, the returns of the timing trading strategy before and after the epidemic are examined, and it can be found that the timing trading strategy has a significant advantage on the risk side. And the return performance of the strategy is unstable in the early stages of the outbreak, suggesting that extreme data have a greater impact on the stability of the strategy.

The results of this paper provide insights into the integration of deep learning methods with econometric methods in the field of asset pricing. In the future, we will try to find more suitable features and build models with stronger forecasting performance.

CRediT authorship contribution statement

Junting Zhang: Methodology, Software, Writing – original draft. **Haifei Liu:** Conceptualization, Resources, Writing – review & editing, Funding acquisition. **Wei Bai:** Methodology, Validation. **Xiaojing Li:** Data curation, Writing – review & editing.

Declaration of Competing Interest

The authors declare that they have no known competing financial interests or personal relationships that could have appeared to influence the work reported in this paper.

Appendix

Table A1 shows the names, abbreviations and markets of the 10 stock index futures used in this paper.

Table A2 lists the names and abbreviations of the models used in this paper.

Fig. A1 shows the process of training the LSTM model on the error sequence generated by ARIMA in the IC sample sequence, from which it can be seen that the error can be reduced more quickly and gradually stabilized, indicating that the training results are better.

Tables A3-A10 demonstrates the evaluation statistics for the in-sample versus out-of-sample prediction results in each time window.

References

Ahmad, M. I., Guohui, W., Rafiq, M. Y., Hasan, M., Chohan, A.-U.-H., & Sattar, A. (2017). Assessing performance of moving average investment timing strategy over the UK stock market. *The Journal of Developing Areas, 51*(3), 349–362.

Bates, J. M., & Granger, C. W. J. (1969). The combination of forecasts. *OR, 20*(4), 451–468.

Bekiros, S., Arreola Hernandez, J., Salah Uddin, G., & Muzaffar, A. T. (2020). On the predictability of crude oil market: A hybrid multiscale wavelet approach. *Journal of Forecasting, 39*(4), 599–614.

Phuong, C. M. (2021). Investor sentiment measurement based on technical analysis indicators affecting stock returns: Empirical evidence on VN100. *Investment Management and Financial Innovations, 18*(4), 297–308.

Phooi, C. (2016). Forecasting east asian indices futures via a novel hybrid of wavelet-PCA denoising and artificial neural network models. *PLoS One1, 11*, e0156338.

Chen, Y.-T., Lai, W.-N., & Sun, E. W. (2019). Jump detection and noise separation by a singular wavelet method for predictive analytics of high-frequency data. *Computational Economics, 54*(2), 809–844.

Choi, J. J. (1995). The Japanese and US stock prices: A comparative fundamental analysis. *Japan and the World Economy, 7*(3), 347–360.

Chortareas, G., Jiang, Y., & Nankervis, J. C. (2011). Forecasting exchange rate volatility using high-frequency data: Is the euro different? *International Journal of Forecasting, 27*(4), 1089–1107.

Dunis, C. L., & Huang, X. (2002). Forecasting and trading currency volatility: An application of recurrent neural regression and model combination. *Journal of Forecasting, 21*(5), 317.

G, C. (2012). Subjective doesn't work in the market: Technical analysis Is the objective standard. Trading Tools and Tactics, 1-15.

Ghahnavieh, A. E. (2019). Time series forecasting of styrene price using a hybrid ARIMA and neural network model. Independent Journal of Management & Production.

Hochreiter, S., & Schmidhuber, J. (1997). Long short-term memory. *Neural computation, 9*(8), 1735.

Høg, E. P. (2001). Non-parametric estimation of diffusion-paths using wavelet scaling methods. *IFAC Proceedings Volumes, 34*(20), 187–189.

Hou, Y., & Li, S. (2020). Volatility and skewness spillover between stock index and stock index futures markets during a crash period: New evidence from China. *International Review of Economics & Finance, 66*, 166–188.

Hu, M. Y., Zhang, G., Jiang, C. X., & Patuwo, B. E. (1999). A cross-validation analysis of neural network out-of-sample performance in exchange rate forecasting. *Decision sciences, 30*(1), 197–216.

Huang, D., Li, J., Wang, L., & Zhou, G. (2020). Time series momentum: Is it there? *Journal of Financial Economics, 135*(3), 774–794.

Islam, S. R., Ghafoor, S. K., & Eberle, W. (2018). Mining illegal insider trading of stocks: A proactive approach. In 2018 IEEE International Conference on Big Data (Big Data) (pp. 1397-1406).

Joo, T. W., & Kim, S. B. (2015). Time series forecasting based on wavelet filtering. *Expert Systems with Applications, 42*(8), 3868–3874.

Juszczuk, P., Kozak, J., & Kania, K. (2020). Using similarity measures in prediction of changes in financial market stream data—Experimental approach. *Data & Knowledge Engineering, 125*, Article 101782.

Kim, H. Y., & Won, C. H. (2018). Forecasting the volatility of stock price index: A hybrid model integrating LSTM with multiple GARCH-type models. *Expert Systems with Applications, 103*, 25–37.

Lin, F.-L., Yang, S.-Y., Marsh, T., & Chen, Y.-F. (2018). Stock and bond return relations and stock market uncertainty: Evidence from wavelet analysis. *International Review of Economics & Finance, 55*, 285–294.

Lin, Y., Yan, Y., Xu, J., Liao, Y., & Ma, F. (2021). Forecasting stock index price using the CEEMDAN-LSTM model. *The North American Journal of Economics and Finance, 57*, Article 101421.

Liu, Z., & Huang, S. (2021). Carbon option price forecasting based on modified fractional Brownian motion optimized by GARCH model in carbon emission trading. *The North American Journal of Economics and Finance, 55*, Article 101307.

Lv, P., Shu, Y., Xu, J., & Wu, Q. (2022). Modal decomposition-based hybrid model for stock index prediction. *Expert Systems with Applications, 202*, Article 117252.

Lv, P., Wu, Q., Xu, J., & Shu, Y. (2022). Stock index prediction based on time series decomposition and hybrid model. *Entropy, 24*(2), 146.

Mejia, J., Avelar-Sosa, L., Mederos, B., Ramírez, E. S., & Díaz Roman, J. D. (2021). Prediction of time series using an analysis filter bank of LSTM units. *Computers & Industrial Engineering, 157*, Article 107371.

Neely, C. J., Rapach, D. E., Tu, J., & Zhou, G. (2014). Forecasting the equity risk premium: The role of technical indicators. *Management Science, 60*(7), 1772–1791.

Novy-Marx, R. (2012). Is momentum really momentum? *Journal of Financial Economics, 103*(3), 429–453.

Pai, P.-F., & Lin, C.-S. (2005). A hybrid ARIMA and support vector machines model in stock price forecasting. *Omega, 33*(6), 497–505.

Persio, L. D., & Honchar, O. (2016). Artificial Neural Networks architectures for stock price prediction: comparisons and applications. In.

Phooi M`ng, J. C. (2018). Dynamically Adjustable Moving Average (AMA') technical analysis indicator to forecast Asian Tigers' futures markets. *Physica A: Statistical Mechanics and its Applications, 509*, 336–345.

Rahimi, Z. H., & Khashei, M. (2018). A least squares-based parallel hybridization of statistical and intelligent models for time series forecasting. *Computers & Industrial Engineering, 118*, 44–53.

Rather, A. M., Agarwal, A., & Sastry, V. N. (2015). Recurrent neural network and a hybrid model for prediction of stock returns. *Expert Systems with Applications, 42*(6), 3234–3241.

Sadorsky, P. (2022). Forecasting solar stock prices using tree-based machine learning classification: How important are silver prices? *The North American Journal of Economics and Finance, 61*, Article 101705.

Shi, Z., & Chehade, A. (2021). A dual-LSTM framework combining change point detection and remaining useful life prediction. *Reliability Engineering & System Safety, 205*, Article 107257.

Shik Lee, H. (2004). International transmission of stock market movements: A wavelet analysis. *Applied Economics Letters, 11*(3), 197–201.

Stevenson, M. J. (1998). Fractal market analysis: Applying chaos theory to investment and economics. *Journal of economic behavior & organization, 34*(2).

Sun, E. W., Chen, Y.-T., & Yu, M.-T. (2015). Generalized optimal wavelet decomposing algorithm for big financial data. *International Journal of Production Economics, 165*, 194–214.

Sun, E. W., & Meinl, T. (2012). A new wavelet-based denoising algorithm for high-frequency financial data mining. *European Journal of Operational Research, 217*(3), 589–599.

Tsang, P. M., Kwok, P., Choy, S. O., Kwan, R., Ng, S. C., Mak, J., … Wong, T.-L. (2007). Design and implementation of NN5 for Hong Kong stock price forecasting. *Engineering Applications of Artificial Intelligence, 20*(4), 453–461.

Wang, Z. m., & Wu, C. (2010). Application of support vector regression method in stock market forecasting. In 2010 International Conference on Management and Service Science (pp. 1-4).

Weytjens, H., Lohmann, E., & Kleinsteuber, M. (2021). Cash flow prediction: MLP and LSTM compared to ARIMA and Prophet. *Electronic Commerce Research, 21*(2), 371–391.

Wright, J. H. (2008). Bayesian Model Averaging and exchange rate forecasts. *Journal of Econometrics, 146*(2), 329–341.

Zhang, G., Eddy Patuwo, B., & Hu, Y. (1998). Forecasting with artificial neural networks: The state of the art. *International Journal of Forecasting, 14*(1), 35–62.

Zhang, G. P. (2003). Time series forecasting using a hybrid ARIMA and neural network model. *Neurocomputing, 50*, 159–175.

Zhu, B., & Wei, Y. (2013). Carbon price forecasting with a novel hybrid ARIMA and least squares support vector machines methodology. *Omega, 41*(3), 517–524.

Zolfaghari, M., & Gholami, S. (2021). A hybrid approach of adaptive wavelet transform, long short-term memory and ARIMA-GARCH family models for the stock index prediction. *Expert Systems with Applications, 182*, Article 115149.